# DEVELOPMENT OF A PROTEIN-BASED THERAPY FOR THE TREATMENT OF SPINAL MUSCULAR ATROPHY

Joseph Burns

A thesis submitted to the

Faculty of Graduate and Postdoctoral Studies

in partial fulfilment of the requirements for the

MSc degree in Biochemistry with specialization in Human and Molecular Genetics

Department of Biochemistry, Microbiology, & Immunology

Faculty of Medicine

University of Ottawa

## Abstract

The autosomal recessive disorder spinal muscular atrophy (SMA) causes motor neuron degeneration and muscle wasting, progressing to paralysis and death in severe cases. The disease is caused by deficiency of survival motor neuron protein (SMN) due to deletion or mutation of the *SMN1* gene. We seek to develop a protein-based therapy for SMA using an adenoviral vector which encodes a secretable form of SMN fused to a protein transduction domain (PTD) derived from the trans-acting activator of transcription (TAT) from HIV. We generated secretable GFP proteins using transient transfection in mammalian cells and determined that the secretory peptide was inefficient when paired with the native PTD. We generated TAT-GFP proteins in bacteria and observed that the variant TAT3 most reliably tranduced cells *in vitro*. We did not observe uptake of the therapeutic protein following infection with an adenoviral vector and subsequent secretion of the protein from infected cells.

**Acknowledgements**

I would like to thank my supervisor, Dr. Robin Parks, for his support and guidance throughout this project. I would also like to thank the members of my thesis advisory committee, Dr. Dennis Bulman and Dr. Rashmi Kothary, for their input and suggestions. I would also like to acknowledge my fellow graduate students, Adam Davidson, Benoit Goulet, Carmen Wong, and Emily McFall, for fruitful discussions and useful advice. In particular, I would like to express my appreciation for Carmen, who reminds me that the sun truly does rise in the East. The assistance and laboratory maintenance provided by the research technicians, Kathy Poulin, Natacha Provost, Kalisa Campbell, and Mélissa Potvin, was important to the progression of this project and I appreciate their contributions. Finally, I would like to thank the government of Ontario for awarding me the Queen Elizabeth II Graduate Scholarship in Science and Technology and thereby funding my stipend for this work.

**Table of Contents**

## List of Abbreviations

ACMG – American College of Medical Genetics
ACOG – American College of Obstetricians and Gynecologists
Ad – adenovirus
ALS – amyotrophic lateral sclerosis
ANS – autonomic nervous system
BBB – blood-brain barrier
BDNF – brain-derived neurotrophic factor
CMV – cytomegalovirus
CNS – central nervous system
CPP – cell-penetrating peptide
ECL – electrochemiluminescence
EIAV – equine infectious anemia virus
ESE – exonic splicing enhancer
ESS – exonic splicing silencer
FBS – fetal bovine serum
GDNF – glial cell-derived neurotrophic factor
GFP – green fluorescent protein
HDAC – histone deacetylase
HIV – human immunodeficiency virus
hnRNP – heterogeneous nuclear ribonucleoprotein
HRMA – high resolution melting analysis
HRP – horseradish peroxidase
IGF-1 – insulin-like growth factor 1
IGFALS – IGF-1 binding protein, acid-labile subunit
IPTG – isopropyl β-D-1-thiogalactopyranoside
ISE – intronic splicing enhancer
ISS – intronic splicing silencer
MEM – minimal essential media
MOI – multiplicity of infection
NMJ – neuromuscular junction
PBS – phosphate-buffered saline
PCR – polymerase chain reaction
PTD – protein transduction domain
RFLP – restriction fragment length polymorphism
RFP – red fluorescent protein
scAAV – self-complementary adeno-associated virus
SDS-PAGE – sodium dodecyl sulfate polyacrylamide gel electrophoresis
SMA – spinal muscular atrophy
SMN – survival of motor neuron (protein)
*SMN1* – survival of motor neuron 1, telomeric (gene)
*SMN2* – survival of motor neuron 2, centromeric (gene)
snRNA – small nuclear ribonucleic acid
snRNP – small nuclear ribonucleic particle
TAT – trans-acting activator of transcription
TGF-α – tumour growth factor α
Unrip – unr-interacting protein
VPA – valproic acid
WHO – World Health Organization
WT – wild-type

## List of Figures

## List of Tables

# Chapter 1 - Introduction

## 1.1: Spinal muscular atrophy

Spinal muscular atrophy (SMA) is an autosomal recessive disease which affects as many as 1 in 6000 live births and has a carrier frequency as high as 1 in 40 people [1-3]. The disease is characterized by degenerative loss of α-motor neurons in the brain stem and spinal cord, which progresses to chronic weakness of trunk and limb muscles and eventually paralysis [3-5]. Thoracic cage deformation and respiratory muscle weakness cause respiratory distress which frequently results in death, particularly in severe cases [6]. Though most patients experience a brief improvement in motor functions and muscular strength following diagnosis, in all cases the disease progresses within 2-3 years following this initial period and never arrests [7]. Severe SMA causes the death of more infants than any other genetic disorder and is currently incurable [1,4]. Appropriately, this disease is the focus of numerous disease pathology and therapeutic research labs all over the world.

## 1.2.: Genetics and SMA

### 1.2.1: Genetic basis

Though there are numerous variations of spinal muscular atrophy, including X-linked SMA [8], distal SMA [9], and scapuloperoneal SMA [10], the most common and most lethal form is termed spinal muscular atrophy 5q13, so named due to its characteristic deletion of the entire survival motor neuron 1 (*SMN1*) gene, which is found on chromosome 5q in band 13 [11,12]. Homozygous deletion of this gene occurs in approximately 95% of SMA 5q13 patients [12], with

the remainder displaying a heterozygous state in which one *SMN1* allele is deleted and the other contains a non-synonymous mutation, or more rarely two *SMN1* alleles which both contain intragenic mutations [13]. The functional loss of *SMN1* results in a deficiency of survival of motor neuron protein (SMN), however the protein is not completely absent in affected patients due to the presence of *SMN2*, a second *SMN* gene present on 5q13 which differs from *SMN1* by five nucleotides [11]. Only one of these point mutations occurs in a coding region: the cytosine found at position +6 of exon 7 in *SMN1* is mutated to thymidine in *SMN2* [14]. Though this is a silent mutation in terms of the amino acid encoded, the change to thymidine at this position results in exclusion of exon 7 from ~90% of *SMN2* transcripts [15]. The protein generated from this incomplete transcript, termed SMNΔ7, is missing 16 amino acids [14,16] which form a domain that is essential for the self-oligomerization of the protein which normally occurs *in vivo* [16,17]. Exclusion of this exon also generates a strong degradation signal at the carboxy terminus of SMNΔ7 that targets the truncated protein to the proteasomal degradation pathway [18]. The instability and vulnerability to degradation renders SMNΔ7 unable to fulfil the functional roles of SMN. A relatively small amount of full-length SMN protein is generated from the 10% of *SMN2* transcripts that include exon 7 [15]. No patients have been identified who have deletions or functional loss of both *SMN1* and *SMN2* [11], suggesting that loss of both genes results in embryonic lethality [19,20]. In the absence of *SMN1*, the full-length SMN generated from *SMN2* is sufficient to prevent embryonic lethality but not sufficient to prevent the degeneration of α-motor neurons and the subsequent presentation of SMA.

Multiple hypotheses exist regarding the exclusion of exon 7 caused by the cytosine to thymidine mutation at position +6 of the exon. Because this exon features weak splicing sites at both the 3' and 5' ends [21], proper inclusion of the exon is dependent on *cis* elements – RNA regions which are recognized by *trans*-acting splicing proteins and thereby enhance the inclusion

or exclusion of a given element in a transcript. These elements include intronic splicing enhancers (ISEs), intronic splicing silencers (ISSs), exonic splicing enhancers (ESEs), and exonic splicing silencers (ESSs). At least one *cis* element from each category is believed to be involved in splicing of exon 7 in *SMN2*. Hofmann *et al* established that exon 7 contains an ESE which binds to the protein Htra2-β1, a positive selector for inclusion [22]. This splicing protein forms a complex with hnRNP-G, hnRNP-Q, and SRP30C which ultimately promotes the inclusion of exon 7 [23]. However, this ESE is not disrupted by the point mutation in *SMN2* and therefore does not fully explain the difference in splicing between the two human *SMN* genes.

Interestingly, a second ESE was identified in the *SMN* genes by Cartegni and Krainer, whose model suggested that the point mutation in *SMN2* disrupts an ESE which is normally associated with the positive splicing protein SF2/ASF [24]. Considering the weak splicing sites present on the exon and its subsequent reliance on *cis*-elements, the loss of an ESE provides a possible causal link between the point mutation and the exclusion of the exon. The actual consequence of this mutation is controversial, however, as a second model proposed by Kashima and Manley suggests that the point mutation actually creates an ESS in that region of the exon [25]. The newly introduced ESS binds hnRNP-A1, a protein-RNA complex which acts as a negative splicing signal. A similar model is presented by Pedrotti *et al*, in which the multifactorial RNA-binding protein Sam68 binds to the mutated region on the pre-mRNA transcript generated from *SMN2* and causes skipping of this exon during transcription (26). Though the exact mechanism is presently unknown, the C to T transition in *SMN2* appears to influence the exclusion of exon 7 from ~90% of transcripts either by disrupting an enhancer site or by generating a new site for the binding of a silencing element on the DNA or the pre-mRNA.

Though the putative changes to *cis* elements caused by the point mutation most intuitively explain the difference in exon 7 splicing between *SMN1* and *SMN2*, many *cis* elements have been

identified on the surrounding introns which may also affect the splicing of the exon. One ISS is present toward the 3' end of intron 6 [27], and another at the 5' end of intron 7 [28]. Three ISEs are present following the ISS on intron 7 [27,29]. Interestingly, an additional ISS is present following these ISEs in *SMN2* only [30], located at position +100 of intron 7. An A to G point mutation generates a new ISS at this site which also binds hnRNP-A1, the same negative splicing protein complex implicated by Kashima and Manley's model for the effect of the C to T transition in exon 7 [30]. Taken together, these observations suggest that intronic *cis* elements in close proximity to exon 7 may also affect its splicing, particularly in the case of *cis* elements newly introduced by point mutations in *SMN2*.

The knowledge amassed to date regarding the genetic basis of SMA has identified potential therapeutic targets and informed the development of *SMN2*-targeting therapeutics. The discovery of multiple *cis* elements in close proximity to exon 7 warrants further investigation. Identifying *SMN1* deletion as the causal origin of the disease has also allowed genetic counsellors and families to make informed family planning decisions after the birth of an affected child.

### 1.2.2: Genetic testing and carrier screening

SMA is a common genetic disease with a very high carrier frequency. Therefore, the prospect of neonatal or even prenatal screening is a topic of debate among clinicians and researchers concerned with SMA. Though the merit of such early screening is controversial, and the necessity of universal screening is debated, carrier screening is presently performed for parents of an affected child in an attempt to predict the prospective disease severity in the next child, if affected [31].

The autosomal recessive nature of SMA necessitates that two unaffected parents who give

birth to an affected child must both be heterozygous carriers of an *SMN1* deletion (or intragenic mutation), except for the rare possibility of a spontaneous mutation in the child which disables *SMN1*, most likely in a child exhibiting heterozygosity for functional *SMN1*. Parents of an affected child are subjected to carrier screening to confirm their carrier status and to assess gene dosage of *SMN2*. If the parents are indeed carriers, their next child has a 25% chance of being afflicted with SMA. Carrier screening is performed by detecting deletions in *SMN1* [32]; however, this presents opportunities for false negatives, as a carrier presenting a loss-of-function intragenic mutation in *SMN1* would be identified as a non-carrier by this screen. Further, a raw quantification of *SMN1* gene incidence can yield a false negative in the case of carriers exhibiting a deletion of *SMN1* on one chromosome and a duplication on the other [32]. Though it is not possible to directly assess disease severity in a presymptomatic patient, the compensatory nature of *SMN2* results in less severe disease in patients with multiple copies of this gene (discussed below) [33]. Therefore, the parents can be screened for *SMN2* copy number in an effort to predict the severity of SMA in an affected child. Presently, screening of the parents of an affected child will confirm carrier status in most cases, but further refinement to account for false negatives is warranted. *SMN2* gene dosage information from the parents may also allow for early establishment of the prognosis for an affected child and allow the parents to prepare accordingly.

Neonates born to confirmed carriers are currently screened for *SMN1* deletion. The most suitable screening method among current technologies for hospital-based testing is likely restriction fragment length polymorphism (RFLP) analysis, in which DNA from the patient is used as a template in a polymerase chain reaction (PCR) using a mismatched reverse primer that introduces a recognition site for the restriction enzyme *Dra*I in the PCR product of *SMN2*, but not *SMN1*. This allows for an unambiguous detection of *SMN1* deletion as the digested fragment corresponding to the *SMN2* PCR product is smaller than the fragment produced by the full-length

*SMN1* PCR product, if present. The absence of the larger band indicates an *SMN1* deletion [34]. This method is appropriate as a diagnostic measure as it does not require specialized equipment and can be performed in one day. However, this method does not detect point mutations resulting in functional loss of *SMN1*, and therefore other diagnostic measures are necessary when the carriers are known to exhibit such mutations. An emerging technology which would allow consideration of *SMN1* point mutations and also assess gene dosage of *SMN2* is high resolution melting analysis (HRMA), in which PCR is performed using an unlabelled *SMN1*-specific probe which complements the guanine present at position -45 of intron 6 in *SMN1* (adenine in *SMN2*) [35]. This PCR will amplify both *SMN1* and *SMN2* if present, but the probe causes the *SMN1* product to be longer and therefore the duplex has a higher melting temperature. High throughput melting curves are then performed on 96-well plates and characteristic curves are generated for patients with *SMN1* deletions, patients with *SMN2* deletions, and for normal patients exhibiting homozygous presence of both genes. Intermediate curves generated for a patient can be used to estimate gene dosage of *SMN2*. This method also permits the detection of intragenic mutations in *SMN1* as mismatches will affect the melting temperature of the duplex [35]. The ability of HRMA to detect deletions and mutations in *SMN1,* ability to estimate gene dosage of *SMN2,* short duration and high throughput capabilities make this assay suitable for population screening.

There is some opposition in the field regarding whether or not genetic screening for autosomal recessive SMA should be performed, primarily due to the limitations of carrier screening and the incurable status of the disease. Opponents of population-based SMA screening cite the significant costs of widespread screening [36], the potential for false negatives in carrier testing [37], and the concern that carrier status testing is only relevant for couples preparing to conceive a child together. SMA carrier status does not affect the health of the individual, and knowing that one is a carrier might render a person hesitant to reproduce without sufficient

education regarding the genetics of the disease. As part of a widespread genetic screen, a carrier might not understand the significance of carrier status when they eventually seek to conceive a child or might not disclose their carrier status to their partner. The prospect of widespread screening is also given pause by the absence of a cure for the disease, particularly in the case of neonatal and prenatal screening. Screening for SMN violates the second of ten criteria adopted by the World Health Organization (WHO) in 1968 (the Wilson-Jungner criteria), which states that in order for a genetic screen to be warranted, "there should be an accepted treatment for patients with recognized disease" [38]. The American College of Obstetricians and Gynecologists (ACOG) cautions against such screening particularly in the prenatal case, as improper understanding of the variability in disease phenotype may lead to poorly informed terminations of pregnancy [39].

On the other hand, due to the high carrier frequency and clinical severity of the disease, the American College of Medical Genetics (ACMG) recommends population-based SMA carrier screening in addition to screening of affected families [2]. While it is true that no accepted treatment for SMA currently exists, the criteria established by Wilson and Jungner were not intended to be dogmatic, but rather to provide a framework for fruitful discussion regarding the ethics of genetic screening [40]. The Wilson-Jungner criteria were written in 1968, long before current screening technologies had been developed which could identify disease in patients before the symptomatic stage. Even in the absence of a cure, early detection of SMN by a neonatal screen could improve quality of life for the patient by allowing the parents to anticipate his or her needs and prepare for the proper care of the affected child [41]. A recent reassessment of the Wilson-Jungner criteria published by the WHO recognized the benefits of genetic screening for disease which lack an accepted treatment and synthesized a new set of tentative criteria based on this consideration and on other new developments in genomics [40]. This proposed set of criteria

does not require a specific established treatment for a disease, but instead requires an established need for the screen, a clear target population, and the integration of patient education in the screening program, none of which are obstacles to SMA screening [40]. Further, *in vivo* studies of SMA therapeutics suggest that early detection is instrumental in affecting phenotypic rescue in mice [42-44]. The therapeutic window for SMA is believed to be early and narrow, therefore early detection is essential to identify candidates for the many therapeutics currently approaching or entering the clinic [3,37]. Though SMA is currently incurable, neonatal screening will be a crucial component of the development of treatments and possibly a cure.

### 1.3: Variable severity and disease types

The reason that genetic screening of a neonate assists in preparing the family for the care of an affected child is that gene dosage of *SMN2* affects severity of the SMA phenotype. Patients exhibiting duplications of *SMN2* experience milder disease and have a greater life expectancy than those without duplications or with *SMN2* deletions [33]. In patients with increased *SMN2* copy number, an additive effect occurs in which the combined full-length transcript derived from each copy of the gene brings the patient closer to the levels of SMN present in an unaffected person. This results in a less severe disease phenotype, as the level of SMN present in a patient is inversely correlated with the severity of symptoms [45,46]. Variability in *SMN2* copy number among patients in turn causes variability in time of disease onset, peak motor function achieved, and life expectancy. These three criteria are used to categorize patients into one of five types of SMA (Table 1.1) [47]. Type 0 is characterized by onset prior to birth, respiratory distress at birth, and very low life expectancy. This type of SMA is fatal if the patient does not receive respirator support upon birth. Type 1, also known as Werdnig-Hoffmann disease, presents before six months

of age. Type 1 patients are unable to sit under their own power and are expected to live for less than two years [48]. In type 2, onset typically occurs between 6 and 18 months of age but may occur sooner. These patients are able to sit independently but never achieve the ability to walk and have life expectancies between 10 and 40 years. Type 3 patients experience disease onset after 18 months and ultimately achieve the ability to walk without assistance. Patients with type 4 SMA first present symptoms at 5 years of age or later and retain the ability to walk. Types 3 and 4 are not associated with a reduced life expectancy [10].

Russman *et al* observed that highest motor function achieved by an SMA patient was more closely correlated to prognosis than age of onset [49]. Among patients with similar ages of onset, those who achieved the ability to sit or to walk independently lived longer than those who did not [49]. This appears to be confounded by a brief period of improvement experienced by most patients following symptom onset [7], during which motor skills may improve before regressing again. However, briefly gaining the ability to walk and then losing it again was still associated with a prognostic advantage over those who never walked [49]. A patient with an earlier age of onset but higher maximum motor function than another patient can be expected to have a greater life expectancy, as the degree of disease progression appears to be more accurately predicted by motor function inhibition.

Quantitative PCR analysis performed by Feldkötter *et al* determined the *SMN2* copy number of 375 SMA patients of known type. The authors generated percent ratios representing the distribution of *SMN2* copy number within each SMA type. Interestingly, the authors also generated percentage ratios that approximate the likelihood of each SMA subtype when the *SMN2* copy number is known (Table 1.1) [50]. The likelihood of an affected child with only one copy of *SMN2* acquiring type 1 SMA is greater than 99.9%. With two copies of the gene, the probability of type 1 SMA is 97.26% , while the probabilities of type 2 and type 3 are 2.7% and 0.04%,

**Table 1.1:** Clinical types of spinal muscular atrophy.

| Type | Age of Onset | Characteristic Motor Function | Life Expectancy | Probability by copy number of *SMN2* (%) | | | |
|---|---|---|---|---|---|---|---|
| | | | | 1 | 2 | 3 | 4 |
| 0 | Before birth | Reduced movement *in utero* | Fatal at birth | -[A] | - | - | - |
| 1 | < 6 months | Sitting,with support | < 2 years | >99.9 | 97.3 | 7.2 | 1.6 |
| 2 | 6-18 months | Independent sitting | 10-40 years | <0.01 | 2.7 | 82.8 | 14.8 |
| 3 | >18 months | Independent walking | Normal | <0.01 | 0.04 | 10.0 | 83.6 |
| 4 | > 5 years | Normal walking | Normal | - | - | - | - |

[A] A dashed line indicates that data was not collected for this type.

respectively. With a copy number of three, type 1 SMA is expected to develop in only 7.2% of cases, with type 2 the most likely at 82.8% and type 3 having a probability of 10%. Finally, in patients with four copies of *SMN2* the expected ratios are 1.6% type 1, 14.8% type 2, and 83.6% type 3 [50]. These ratios present *SMN2* copy number as an imperfect predictor of phenotypic severity, particularly if the screen used does not account for intragenic mutations within some copies of *SMN2* or incomplete duplications. The study also did not include patients with SMN type 4 and could not include type 0 patients due to their short life expectancy. Neonatal screening for *SMN2* copy number could serve to prepare parents of an affected child for the necessary care of the child and inform their expectations regarding motor function and life expectancy. However, clinical evaluation following symptom onset will provide a more accurate answer for such concerns.

## 1.4: SMN protein and putative functions

### 1.4.1: The SMN complex

The survival motor neuron protein is a 38 kDa protein which is ubiquitously expressed and is found in both the cytoplasm and the nucleus [51,52]. Full-length SMN self-oligomerizes via association of a 30-amino acid domain encoded by exon 6 [16]. The self-association appears to be dependent on the presence of amino acids that follow this domain, which are absent in the product of most *SMN2* transcripts [16]. Following self-oligomerization, nuclear SMN is recruited into a macromolecular complex containing gemin proteins. The formation of this complex appears to have a stabilizing effect, and failure to self-oligomerize or to be recruited into these complexes may explain the reduced half-life of SMNΔ7 compared to the full-length protein [17]. The SMN complex is composed of SMN and Gemins 2 through 8 [53]. The name for the associated

proteins is derived from Gemini, as the nuclear structures resembled twins of other previously identified coiled bodies in the nucleus [51]. The cellular localization of the complex appears to be influenced by its interaction with unr-interacting protein (Unrip), which directs localization to the cytoplasm and is absent in nuclear gems [54].

### 1.4.2: snRNP assembly and pre-RNA splicing

The SMN complex is known to play a role in the assembly of small nuclear ribonucleoproteins (snRNPs) [55], which are complexes composed of small nuclear RNA (snRNA) and Sm proteins which combine to form spliceosomes [56,57]. Gemin 5 has been found to be essential to this function of the SMN complex [58]. This protein features 13 tryptophan-aspartic acid (WD) repeats at its N terminus which cause it to bind the 3' end of snRNA molecules [58]. Splicing-associated Sm proteins bind directly to other proteins in the SMA complex and are combined with the snRNA to generate snRNPs [53,57,59]. The tudor domain of SMN appears to function in snRNP assembly by binding Sm proteins required in the snRNPs [57]. Depletion of SMN in a given cell results in a corresponding decrease in the cell's ability to assemble snRNPs [55], suggesting that the role of SMN in binding Sm proteins and as a structural element of this complex are important for snRNP assembly and, ultimately, splicing. This raises the question of why such a general function performed by a ubiquitous protein results in the degeneration of only α-motor neurons. Since the establishment of snRNP assembly as a functional role of SMN, much research has been undertaken to elucidate how this function may relate to the disease phenotype and to determine other functions of the protein. Gabanella *et al* observed a correlation between snRNP assembly impairment and disease severity in SMA mice [60]. In contrast, a study performed in zebrafish by Carrel *et al* depleted SMN in the animals using morpholinos and

injected RNA corresponding to numerous *SMN* mutants and observed their effect on motor axon phenotype [61]. The authors observed that some of their mutant RNAs restored self-oligomerization and snRNP assembly, but failed to correct the motor axon phenotype [61]. These results suggest that the SMA disease phenotype is not caused by decreased snRNP assembly but by loss of some other function of SMN.

The role of SMN in snRNP assembly may have direct consequences for pre-mRNA splicing. The association between SMN and splicing was first observed by Pellizzoni *et al*, who demonstrated that a dominant negative SMN mutant inhibited pre-mRNA splicing *in vitro*, versus wild-type SMN which enhanced splicing [62]. The authors also assayed SMN mutants derived from SMA patients and found that these proteins failed to stimulate pre-mRNA splicing [62]. These observations generated interest in assessing splicing defects as a pathway for SMA pathogenesis. Zhang *et al* depleted SMN in cells using an inducible shRNA system and observed the effect on snRNP assembly and the specific snRNP profile generated. When SMN levels were reduced to approximately 15% of normal, snRNP levels were significantly reduced in a manner that did not affect all snRNPs equally and was characteristic for each cell type [63]. The authors hypothesized that such cell-specific snRNP disruption might have tissue-specific consequences to splicing. Brain, spinal cord, and heart samples recovered from SMA mice displayed significant reduction in the minor spliceosomal snRNPs [63], consistent with the findings of Gabenella and colleagues [60]. Interestingly, samples from brain, spinal cord, and kidney of SMA mice displayed widespread aberrant splicing at the peak of disease progression in which genes containing multiple introns were frequently spliced incorrectly [63]. These observations provide a possible link between a general function of SMN and a tissue-specific disease. However, exon-array analysis of SMA mice across three time points – pre-symptomatic, early symptomatic, and post-symptomatic – indicated that little aberrant splicing occurred until the post-symptomatic

stage [64]. Though the possibility remains that the few transcripts that show incorrect splicing at earlier time points may be important for SMA pathogenesis, no causal link has been established for these transcripts. Therefore, splicing defects appear to be a secondary effect of SMN deficiency. Such defects may prove to be clinically important in later phases of the disease but do not appear to be the causative pathway.

### 1.4.3: Active transport and axon outgrowth

With no clear connection between the housekeeping functions of SMN and the disease pathogenesis, some researchers began to focus on other putative functions of SMN which may explain the specific degeneration of α-motor neurons. Fan and Simard established that SMN localized in growth cones during differentiation of murine embryonal teratocarcinoma cells into neurites [65]. This localization was later determined to be exon 7-dependent, further implicating axon growth abnormalities in SMA pathogenesis [66]. Cytoplasmic SMN complexes are found in actively transported granules and contain the gemin proteins, but not Sm proteins [67], indicating that this function of SMN is independent from its role in snRNP assembly. Instead, SMN appears to associate with heterogeneous nuclear ribonucleoprotein (hnRNP) R, which in turn binds β-actin mRNA [68,69]. The interaction between hnRNP R and β-actin RNA is dependent on the association of SMN with the RNP [68]. Ting *et al* recently observed that cytosolic SMN is associated with the coatamer protein Cop-α and is found in Golgi-associated secretion vesicles [70]. Together, these observations suggest that SMN granules associated with hnRNP R and β-actin mRNA are secreted from the Golgi and travel to the growth cones of axons. Trafficking of β-actin mRNA to growth cones allows for β-actin synthesis and subsequent extension of the axon. This model is supported by the observation of decreased levels of hnRNP R and β-actin along the

axons and in growth cones of SMN-depleted cells [68]. In theory, disruption of this trafficking function would cause incomplete extension and improper polarization of neuronal axons. Indeed, disruption of Golgi-mediated granule secretion *in vitro* caused growth cone defects similar to those observed in SMN knockdown cells [70]. Recent work by Fallini *et al* suggests that the tudor domain of SMN interacts with HuD, a poly(A) mRNA binding protein, and SMN may thereby participate in transporting other mRNAs to axons [71]. Depletion of SMN was found to inhibit motor axon outgrowth and pathfinding in a zebrafish model of SMA [61,72], though no such axonal defects were observed in post-symptomatic SMA mice [73]. Thus, the data from animal models appear to conflict regarding whether or not axonal transport defects contribute to disease pathogenesis.

### 1.4.4: Translational regulation

In addition to regulating protein expression at the mRNA level, SMN may also have a role in translational repression. Sanchez *et al* observed up-regulation of the arginine methyltransferase CARM1 in the spinal cords of SMA mice and in patient-derived fibroblasts [74]. Consistent with a previously established regulatory pathway in motor neurons [75], SMN appears to inhibit translation of CARM1 mRNA, likely via its interaction with HuD, as a point mutation in the Tudor domain completely eliminated the translational repression capability of SMN [74]. The identification of an mRNA which is translationally regulated by SMN expands the scope of pathological implications of SMN deficiency.

### 1.4.5: Cytoskeletal integrity and the neuromuscular junction

In addition to its role in active transport to axons, SMN appears to have important functions in the cytoskeletal integrity of neurons [76,77] and in proper formation of the neuromusuclar junction [5,78,79]. SMN depletion causes increased availability of profilin IIa, a protein which normally interacts with SMN in neurons. The increase in profilin IIa availability results in abnormally high levels of the ROCK/profilin IIa complex, which in turn activates the RhoA/ROCK actin remodelling pathway [76]. The improper activation of this pathway causes cytoskeletal instability; however, depletion of profilin IIa in phenotypic neurons does not correct the phenotype, suggesting that other actin remodelling pathways are involved [77]. At the neuromuscular junction (NMJ), synapses of neurons come within close proximity of motor endplates of muscle fibres to allow the passage of vesicles from the neuron to the muscle fibre across the synaptic cleft [80]. In severe SMA mice (*Smn*$^{-/-}$*; SMN2*), many motor endplates were found to have abnormal morphology and to be denervated or only partially innervated [78]. A similar study in a less severe mouse model of SMA (*Smn*$^{2B/-}$) verified that the apparent denervation occurred following the formation of synapses and was not due to a failure in synaptic growth and is independent from defects in axonal growth [79]. While developing a *Drosophila* model for SMA, Chang *et al* observed localization of SMN in the motor endplates of muscle fibres [81], suggesting that there may a role for SMN in motor endplate maturation. Therefore, multiple functions have been identified for SMN which may explain why deficiency of this protein results in a neuromuscular disease. Further investigation is underway to determine which of these functions is responsible for SMA pathogenesis so that therapeutic targets can be identified.

### 1.4.6: Roles for SMN in peripheral tissues

The ubiquitous expression of SMN implies that deficiency of the protein may have other consequences that are not immediately obvious in severe SMA patients due to their short life expectancy. SMN starts to be expressed in mouse embryos 5.3 weeks into gestation and is found at high levels in most tissues including skeletal muscle, spinal cord, spleen, heart, kidney, liver, and lungs [82]. The expression pattern of SMN is similar across all stages of embryonic development [82]; however, expression in tissues other than the brain and spinal cord decreases substantially after embryogenesis in rats [83], which suggests that SMN is less important in these tissues once embryogenesis has completed. The ubiquitously high levels of SMN expression during development may indicate an important function for SMN during development in peripheral tissues. Deficiency of SMN in these tissues may have consequences that are not immediately apparent in patients with severe SMA. The contribution of *SMN2* to the pool of full-length SMN was observed to be greater in muscle and kidney compared to the spinal cord [84], suggesting that *SMN2* is more effective at preventing disease phenotype in peripheral tissues than in α-motor neurons. Considering that peripheral tissues appear to have lesser need for SMN, *SMN2* may be able to compensate for the deletion of *SMN1* in these tissues, particularly in patients with a higher *SMN2* copy number. In patients with fewer copies of *SMN2*, symptoms in peripheral tissues may not manifest due to the early mortality of the disease.

Congenital heart defects are closely associated with severe SMA [85]. A clinical study by Rudnik-Schöneborn *et al* sought to establish whether or not congenital heart defects previously reported in SMA type 0 (one copy of *SMN2*) patients were coincidental. The authors observed congenital heart defects in three of four type 0 patients (75%). The probability of a congenital heart defect and type 0 SMA occurring in the same individual by chance alone is less than 1 in 50 million, implicating a role for SMN in proper development of the heart [85]. This observation is

supported by *in vivo* studies in which structural and functional abnormalities were found in the hearts of mice from two SMA models across three different labs [86-88]. A retrospective analysis of 37 SMA patients exhibiting type 2 or type 3 disease revealed that all but two patients had normal heart function as measured by several parameters. The remaining two patients had dilation of the left ventricle caused by coronary heart disease and hypertension [89]. These observations suggest that compensation by *SMN2* is sufficient to prevent defects in the heart in patients with higher copy numbers, but insufficient in patients with only one copy of the gene. This presents an apparent disease characteristic caused by *SMN1* deletion in a tissue outside of the central nervous system (CNS) and highlights the possibility that others may exist.

In addition to its effect on the central nervous system, deficiency of SMN may also have consequences for the autonomic nervous system (ANS). Some of the observed cardiac defects such as bradycardia and blood pressure fluctuations appear to be the result of ANS dysfunction [90,91]. While examining defective hearts of SMA mice, Heier *et al* noted reduced innervation of the heart in SMA mice compared to age-matched littermates [88]. Other conditions observed in SMA patients which implicate ANS damage include unusual vasodilation responses to cold and necrosis of fingers and toes [91,92]. These ANS abnormalities have been observed in type 1 SMA patients, suggesting that compensation by *SMN2* in the ANS may be poorer than in cardiac tissue. Like cardiac tissues, the ANS appears to be largely unaffected in patients with type 2, type 3, or type 4 SMA. The prospect of ANS damage caused by SMN deficiency suggests that SMN may be essential to other neurons as well, if in lesser quantities.

Some evidence suggests that SMN deficiency affects skeletal muscle directly in addition to causing its denervation. Martinez-Hernández *et al* compared skeletal muscle from type 1 SMA patients to age-matched controls and found that the myotubes in the SMA patient samples were smaller and less organized. These observations suggest that muscular growth and maturation is

delayed in severe SMA [93] and are consistent with a prior *in vitro* study in which SMN-depleted C2C12 myoblasts generated malformed myotubes and had difficulty fusing [94]. Interestingly, the effect of SMA on skeletal muscle does not appear to be uniform [95]. The most severely affected muscles in the SMNΔ7 mouse model are analogous to the most clinically relevant muscles in humans. However, this specificity appears to be due to NMJ defects rather than abnormal muscular growth, as these muscles are fully innervated at postnatal day 1 but become largely denervated by postnatal day 4 [95]. Therefore the loss of function of these specific muscles appears to be caused by loss of the synapse at the NMJ rather than improper development of the muscle or the NMJ [79,95]. However, it is possible that abnormal muscle growth occurs in SMA in addition to denervation of skeletal muscle. Recently, Hayhurst *et al* extracted muscle-resident stem cells known as satellite cells from severe SMA mice and their wild-type littermates. The two populations of satellite cells displayed similar proliferative potential and survival, but the satellite cells derived from the SMA mice encountered difficulty during differentiation resulting in inefficient myotube formation [96]. This suggests that SMN deficiency directly harms skeletal muscle formation. Thus, the skeletal muscle phenotype of SMA appears to be a primary symptom which is compounded by the death of motor neurons and defects in the NMJ.

The SMN protein may also play a role in metabolism. A clinical study by Crawford *et al* compared the plasma levels of the fatty acids dodecanoic acid and tetradecanoic acid among severe SMA patients to healthy controls and to infants with similarly debilitating denervation disorders [97]. The plasma levels of these fatty acids were significantly higher in severe SMA patients than in either control group, indicating that the aberrant fatty acid metabolism is not due to denervation or muscular atrophy alone. Severe SMA patients also exhibited dicarboxylic aciduria when fasted, and yielded urine fatty acid profiles similar to those observed in patients with mitochondrial disorders. Autopsy of some severe SMA patients revealed fatty vacuolization

of the liver, which is characteristic of fatty acid oxidation disorders [97]. Therefore, aberrant fatty acid metabolism in SMA appears to be independent of motor neuron loss and muscular wasting. SMA patients with less severe disease exhibited normal fatty acid metabolism [97]. Recent work by Bowerman *et al* reported pancreatic defects in the $Smn^{2B/-}$ model, specifically an excess of glucagon coupled with decreased levels of insulin [98]. Examination of the pancreatic islets revealed an abnormally high level of glucagon-producing $\alpha$ cells and a diminished representation of insulin-producing $\beta$ cells, resulting in fasting hyperglycemia and glucose resistance in the mice [98]. The abnormalities observed in the murine pancreata were reflected in autopsy samples from severe SMA patients, some of whom had a recorded history of glucose resistance [98]. These two studies indicate that SMN deficiency may have far-reaching consequences for metabolism.

As more functions for SMN are discovered across a wide variety of tissues, interest grows in the restoration of SMN to all tissues rather than strictly to the CNS. A study of transgenic mice with doxycyclin-induced SMN expression revealed that long-term, neural tissue-specific induction of SMN beginning at postnatal day 1 rescued the phenotype, but 70% of the mice died within a month once the induction was ceased after 28 days. The neuromuscular junctions of these animals appeared to be normal at the time of death, which implies that the absence of SMN in another tissue was ultimately the cause of death [99]. Underscoring the importance of SMN in peripheral tissues is a study by Hua *et al* in which an antisense oligonucleotide designed to correct the aberrant splicing in *SMN2* transcripts was injected into the CNS, subcutaneously, and/or systemically. Systemic injection yielded much greater phenotypic rescue than injection of the CNS [100]. Thus, restoration of SMN in peripheral tissues in addition to the CNS may prove instrumental in the development of a cure for SMA.

## 1.5: Emerging therapy for SMA

### 1.5.1: Introduction

The genetic basis and phenotypic effects of SMA allow for three areas of focus for therapeutic development. The first is to attempt to correct the aberrant splicing of the *SMN2* gene product or to stabilize the Δ7 protein. Alternatively, the downstream damage caused by SMN deficiency can be addressed by protecting affected tissues from toxicity and ultimately from death. The third approach is to reintroduce the missing *SMN1* gene or its gene product using a therapeutic vector. Within each of these strategies there exists a wide variety of therapeutics in development, some of which have entered clinical trials.

### 1.5.2: *SMN2*-targeting agents

Targeting the splicing defect in *SMN2* is an avenue which capitalizes on the presence of workable genetic material within the patient and may amplify the effect of the therapeutic in patients with higher *SMN2* copy number. Therapeutics of this nature seek to overcome the obstacles present within *SMN2* which lead to frequent excision of exon 7. The histone deacetylase (HDAC) inhibitor sodium butyrate was found to increase the production of full-length SMN *in vitro* and increased lifespan in SMA mice [101]. Decreased deacetylation of histones appears to alter the splicing pattern of the *SMN2* transcript rather than simply increasing SMN output [101]. Another HDAC inhibitor, valproic acid (VPA) has a similar effect on *SMN2* splicing [102,103]. Presently in use to treat epilepsy, VPA was shown to increase the level of SMN in phenotypic fibroblasts by activating *SMN2* transcription and correcting exon 7 excision [102,103]. Treatment with VPA increased the levels of splicing factors Htra2-β1, SF2/ASF and Srp20, which may partly

explain the correction of the splicing defect and may have implications for the use of VPA in other splicing-related disorders [103]. A clinical study in which SMA type 3 and type 4 patients were treated with VPA for 8 months reported increased muscle strength [104]. An open label study in SMA type 2 patients conducted by Swoboda *et al* concluded that VPA could ameliorate motor function defects, however nearly all patients who exhibited a significant response were under 5 years of age [105]. A double-blind, placebo controlled followup of this study reported no significant improvement in patients who were treated with VPA for 6 to 12 months [106]. The variation between these two studies was later attributed to the existence of responders and non-responders to VPA treatment: increased expression of the fatty acid translocase CD36 appears to nullify the effectiveness of VPA in a large fraction of patients [107]. Nonetheless, early clinical success with VPA indicates that further investigation into therapeutic HDAC inhibitors is warranted.

HDAC inhibitors are not the only drugs that increase levels of full-length SMN. Early studies in SMA type 2 patients indicated that the β-adrenergic agonist salbutamol enhanced muscle performance when administered orally every day for 12 months [108]. A similar study also observed significantly increased levels of full-length *SMN2* transcript in patient leukocytes after 6 to 12 months of treatment [109]. Treatment with the hormone prolactin was also shown to increase the levels of SMN protein and partially rescue phenotype in a mouse model of SMA by activating the STAT5 pathway [110]. Interestingly, systemic administration of prolactin also increased SMN expression in the brain and spinal cord of wild-type mice [110]. Though salbutamol requires long-term dosing and prolactin carries the risk of reproductive side effects [110], these drugs present new mechanisms by which the SMA phenotype may be alleviated.

Considering the presence of ISS elements in close proximity to exon 7 [27-30], and the possibility that the point mutation in *SMN2* exon 7 may disrupt an ESE [24] or introduce an ESS

[25], many oligomer-based therapeutics are in development which interact with these elements to correct *SMN2* splicing. One such strategy uses bifunctional oligonucleotides in which the midsection consists of a sequence of nucleotides that is antisense to part of the *SMN2* gene while each end contains ESE motifs to promote inclusion of the exon [111]. Treatment of SMA mice with these oligonucleotides resulted in significantly improved weight gain, muscle function, and lifespan over untreated littermates; however, the oligonucleotide was introduced via germline transgenesis, raising questions regarding its clinical applicability [111]. Another strategy employs *trans*-splicing of virally-introduced RNA corresponding to part of intron 6 and the complete exon 7 from SMN1, with two hemagglutinin epitopes and a polyadenylation signal at the 3' end. The RNA binds to intron 6 of *SMN2* pre-mRNA via complementary base-pairing and is spliced into the *SMN2* transcript, resulting in a transcript that contains exon 7 [112,113]. Though the *trans*-spliced transcript lacks exon 8, its presence still extended survival in severe SMA mice by approximately 70% [113]. More recent iterations of these RNAs have included an antisense section that blocks the downstream splice site of exon 7 and a section encoding the neurotrophic factor insulin-like growth factor 1 (IGF-1), which has been shown to reduce neuron and muscle cell death in SMA mouse models (discussed below) [86]. These enhanced *trans*-splicing oligonucleotides significantly increased SMN expression in the brain and spinal cord when injected intracerebroventricularly and increased both the lifespan and body mass of severe SMA mice [86]. A third antisense olignucleotide-based approach targets the ISS in intron 7 [114]. Masking of this ISS using a complementary DNA oligonucleotide results in a high degree of exon 7 inclusion [114]. A followup study using an optimized antisense oligonucleotide delivered by infusion to a lateral cerebral ventricle induced increased exon 7 inclusion and prevented tail and ear necrosis in severe SMA mice [115]. Intracerebroventricular injection of the oligonucleotide was shown to increase full-length SMN levels in motor neurons of SMA mice [116]. These

oligonucleotide-based therapeutics present a promising strategy as they continue to progress toward clinical study. An antisense oligonucleotide therapeutic developed by Isis Pharmaceuticals and Biogen Idec has entered clinical study, beginning with a phase I trail in 28 patients [3]. The agent was well tolerated and appeared to improve motor function in some of the treated patients [3,117].

Though the SMN protein is unstable when exon 7 is excluded [16-18], elevated levels of SMNΔ7 protein extend the lifespan of SMA mice, evidenced by the increased longevity of the SMNΔ7 mouse line [118] This mouse line is similar to the severe SMA model in that the mice are homozygous for deletion of murine *Smn* and contain two copies of human *SMN2*, but the addition of homozygous *SMNΔ7* expression in these mice extends average lifespan from 5.2 to 13.3 days [118]. Therefore, elimination of the strong degradation signal found at the carboxy terminus of SMNΔ7 [18] and the presence of amino acids following exon 6, an apparent requirement for self-oligomerization [16], may yield stable protein capable of performing functions of SMN even in the absence of exon 7. Aminoglycosides, a class of drugs that affect translation, have been used with success to extend translation of the Δ7 transcript beyond the stop codon, resulting in a more stable SMNΔ7 protein [119]. Two of these drugs have entered *in vivo* study in SMA mice: TC007, which increases ventral horn cell number and lifespan when introduced directly to the CNS [120,121]; and G418, also known as geneticin, which improved motor function when injected intraperitoneally, but did not increase lifespan due in part to drug-related toxicity [119]. These read-through drugs present an interesting case for the stabilization of the carboxy terminus of SMNΔ7 as a therapeutic strategy; however, the importance of exon 7 in cytoplasmic localization of SMN [66] means that complete amelioration of symptoms with such a therapeutic is unlikely.

### 1.5.3: Non-SMN targets

Therapeutics with non-SMN targets may help to rescue the disease phenotype with or without restoration of SMN. Neuroprotective therapeutics have proven effective in amyotrophic lateral sclerosis (ALS), another incurable disease of motor neurons [122]. Specifically, a class of drugs known as β-lactam antibiotics has been shown to protect neurons from glutamate toxicity by increasing the amount of the glutamate transporter GLT1 [122]. Glutamate toxicity is believed to contribute to progressive motor neuron loss in ALS [123] and thus may have a role in neuron degeneration in SMA. Nizzardo *et al* administered the β-lactam antibiotic ceftriaxone to SMNΔ7 mice by intraperitoneal injection and observed a marked improvement in body mass, motor neuron count, NMJ condition, and muscle strength in treated animals versus control littermates [124]. The authors concluded that the neuroprotective effect appeared to be multi-mechanistic, as they observed increased levels of not only GLT1 but also the transcription factor Nrf2 and, interestingly, SMN protein [124].

IGF-1, a protein implicated in proliferation, survival, and growth [125], is emerging as a protein of interest for SMA therapeutics. Hua *et al* observed that neonatal SMA mice exhibited decreased expression of IGF-1 binding protein, acid-labile subunit (IGFALS), in the liver, resulting in a decrease in circulating IGF-1 compared to control mice and thereby establishing a tentative role for IGF-1 in SMA pathology [100]. The inclusion of IGF-1 in the enhanced *trans*-splicing RNA mentioned previously [86] appeared to improve the corrective effect of that therapeutic, but the effect that can be attributed to IGF-1 alone is difficult to determine from these results [86]. Tsai and colleagues injected viral vectors enclosing human IGF-1 cDNA into the dorsal cochlear nucleus of severe SMA mice [126]. The treated mice displayed a significant reduction in motor neuron cell death compared to controls, but this did not translate to improved motor function [126]. SMNΔ7 mice featuring a muscle-specific rat IGF-1 transgene displayed

increased muscle mass over control littermates, but again this reduction in cell death did not result in improved motor function [127]. The commercial drug IPLEX (recombinant human IGF-1 complexed with human recombinant IGF binding protein 3) appears to improve motor function, increase muscle size, and decrease the amount of neuronal degeneration in SMNΔ7 mice when injected IP starting at P1 [128]. However, IPLEX administration did not increase lifespan or body weight, and the restoration of motor function was far from complete [128]. Taken together, these results suggest that IGF-1 may be effective in preventing cell death in the spinal cord and skeletal muscle, but reducing cell death in these tissues is not sufficient to improve motor function. IGF-1 may be a useful component of a therapeutic construct but does not appear to rescue the SMA phenotype on its own.

In response to their observation that the RhoA/ROCK actin remodelling pathway is overactive in SMA [76,77], Bowerman *et al* assessed the efficacy of two ROCK inhibitors – Y-27632 [129] and fasudil [130] – in the $Smn^{2B/-}$ model. The authors observed that both ROCK inhibitors extended lifespan, increased muscle fibre size, and improved the condition of NMJs via a mechanism independent from SMN restoration [129,130]. Though effective in the intermediate model, Y-27632 did not extend survival in a model of severe SMA, suggesting that ROCK inhibitors may be better suited for less severe cases of the disease (129).

### 1.5.4: Replacement of *SMN1*

An intuitive approach for correcting a disease caused by deletion of a gene is to reintroduce that gene or its product. In the context of SMA, many groups have developed therapeutic strategies that seek to reintroduce *SMN1* using stem cell transplantation or viral vectors. Transplantation of neural stem cells derived from the spinal cord into the intrathecal

space of SMA mice resulted in improvements in lifespan and function [131]. The stem cells exhibited appropriate migration and generated a small number of mature motor neurons. The improvements in phenotype were too great to be attributed to the transplanted neurons alone, and it appears that the transplantation caused a widespread shift in SMN expression toward the wild-type pattern, changes in RNA processing, and increased actin stability [131]. A second study by the same group assessed the effect of embryonic stem cell-derived neural stem cell administered in the same manner [132]. These stem cells demonstrated similar success in improving the SMA phenotype, in part by secreting neuroprotective factors such as tumour growth factor (TGF)-α, glial cell-derived neurotrophic factor (GDNF), and brain-derived neurotrophic factor (BDNF) [132]. Together, these data present a promising strategy to SMA treatment using stem cells from multiple sources.

Viral vectors allow for the introduction of *SMN1* and other transgenes while utilizing interesting viral properties such as retrograde transport. Azzouz *et al* designed a gene therapy vector based on the lentivirus equine infectious anemia virus (EIAV) that contained a human *SMN1* transgene and injected it into various muscles of SMNΔ7 mice [133]. The authors observed improvements in body mass, lifespan, SMN expression in neurons, and motor neuron preservation. Retrograde delivery of the vector was verified by the detection of gems in the nucleus of spinal cord motor neurons which were not detected in control treated littermates [133]. Another gene therapy vector that has had success *in vivo* is self-complementary adeno-associated virus (scAAV) 8 [116]. Self-complementary AAVs are so named for their double-stranded DNA genome which allows for earlier expression of the transgene compared to AAVs with single-stranded genomes [3]. SMNΔ7 mice were injected at birth with a scAAV8 containing a human SMN transgene in their cerebral lateral ventricles. SMN expression was enhanced substantially throughout the spinal cord, and treated mice exhibited improved muscle strength, lifespan, body

mass, and NMJ architecture [116]. A similar vector, scAAV9, was equipped with an *SMN1* transgene and delivered intravenously to SMNΔ7 mice at postnatal day 1, 5, or 10. Intervention at postnatal day 1 resulted in significant improvement in lifespan and body weight, and nearly identical motor performance compared to wild-type littermates. Injection at postnatal day 5 resulted in only partial rescue of the phenotype, with virtually no effect discernible in mice treated later than postnatal day 5 [43]. These results highlight the early and brief therapeutic window in mice which likely requires similarly early treatment in humans. The same vector was shown to improve lifespan and disease phenotype in a more severe model of SMA when introduced at postnatal day 1 [44], suggesting that perinatal or perhaps even prenatal gene therapy may be effective in severe SMA patients. In addition to the temporal restrictions to their effectiveness, there is concern that scAAV vectors may not be viable for use in older patients with less severe SMA because antibodies against AAV capsids are quite common in human populations, with ~40% of healthy adults seropositive for anti-AAV8 IgG antibodies and ~45% seropositive against AAV9, two of the more promising AAV serotypes [134]. In the context of perinatal treatment of SMA, these vectors are still likely to be effective as the newborn patient is unlikely to have encountered any AAV serotypes prior to treatment [43]. Therefore, virally-mediated gene therapy remains an interesting option for treatment of severe SMA.

Direct replacement of SMN protein is rarely considered when designing SMN therapeutics because the protein does not normally cross plasma membranes, presenting an obstacle to therapeutic delivery. Therefore, effective delivery of exogenous SMN to motor neurons and other tissues would require fusion of SMN to a cell-penetrating peptide (CPP). CPPs are highly basic, arginine-rich domains which signal a protein for uptake by macropinocytosis [135,136]. The cell penetration capability of the trans-acting activator of transcription (TAT) protein from the HIV virus was first reported 25 years ago [137], and was later attributed to a

short CPP rich in basic amino acids [138]. This basic domain was required for the rapid uptake of truncated TAT proteins, allowing transduction of the viral protein into the cell and accumulation in the nucleus [138]. For this reason, these domains are also called protein transduction domains (PTDs). Fusion of therapeutic proteins to the PTD from HIV TAT became an area of interest for protein therapeutics, even for particularly large therapeutic proteins. Using the TAT PTD, Schwarze *et al* succeeded in delivering β-galactosidase, a 120 kDa protein, across the blood-brain barrier (BBB) [139], when delivery across the BBB was previously thought to be limited to molecules with a molecular weight of 500 Da or less [140]. The success of this study spurred interest in the use of TAT PTD to treat diseases of the CNS. Cao *et al* employed a fusion of TAT to Bcl-xL, a known death-suppressing molecule, in a mouse model of ischemic brain injury [141]. Neurons in the treated mice were transduced by the fusion protein within two hours of intraperitoneal injection and protected against apoptosis in ischemic neurons [141]. In a muscular disease context, TAT was successfully used to delivery full-length and truncated versions of utrophin, a dystrophin analogue, in a mouse model of Duchenne muscular dystrophy [142]. Fusions of TAT and the truncated utrophin successfully transduced all the tissues collected for analysis and alleviated motor dysfunction and muscle cell degeneration [142]. Successful delivery of TAT fusion proteins across the BBB and to a variety of tissues including skeletal muscle makes TAT-SMN an appealing prospect for SMA therapy.

Another limitation on the effectiveness of protein therapy is the frequent dosing required to maintain sufficient protein levels. One approach to circumvent this limitation is to modify cells within the patient to express and secrete the therapeutic protein. Flinterman *et al* demonstrated that TAT-GFP generated in a producer cell population could be secreted by those cells and subsequently taken up by recipient cells, when appropriate modifications were made to the TAT-GFP [143]. Responding to concern that cleavage of the TAT PTD would occur during secretion

via the ER/Golgi pathway, the authors modified the PTD to remove two furin recognition sites without compromising the protein transduction capability of the domain [143]. The protein was also attached to a signal peptide which marks it for secretion. Efficient GFP uptake was observed in recipient cells co-cultured with producer cells expressing the secreted form of the fusion protein, but not in recipients co-cultured with cells producing the non-secreted control [143]. The results of this study and of the previously mentioned studies using TAT fusion proteins suggest that a TAT-SMN fusion could be secreted from a producer cell population *in vivo* and transduce α-motor neuron and peripheral tissues, possibly rescuing the disease phenotype.

### 1.6: Rationale

SMA is a disease of SMN deficiency. Restoration of SMN protein levels in α-motor neurons and in peripheral tissues has been shown to ameliorate the disease phenotype and extend lifespan in SMA mice. Further, treatments reported to increase SMN levels *in vitro* have improved motor function and muscle strength in human patients. Protein therapy can reintroduce proteins to deficient individuals. In order to cross cell membranes, proteins can be fused to the TAT PTD. To effect long-term production of a therapeutic protein, a producer cell population can be modified to generate a secreted therapeutic protein. The producer cells can express the fusion protein and secrete it, allowing for systemic delivery of the therapeutic protein. Systemically delivered TAT fusion proteins can cross the BBB and be taken up by neurons. In the present study I sought to develop a protein therapy approach in which hepatocytes are infected with an attenuated adenovirus encoding a secreted TAT-SMN protein.

### 1.7: Hypothesis

A furin-resistant, secreted TAT-SMN fusion protein encoded by an adenovirus can be secreted by producer cells and transduce uninfected recipient cells.

### 1.8: Objectives

The specific aims designed to test this hypothesis are: (i) to assess secretory peptide function using transient transfection of SP-GFP fusions, (ii) to compare TAT PTD variants by treating cells with bacterially generated TAT-GFPs, and (iii) to generate adenoviral vectors delivering a secretable TAT-SMN fusion.

# Chapter 2 – Materials and Methods

## 2.1: Constructs

Plasmids encoding TAT-GFPs intended for expression in mammalian or bacterial systems and plasmids encoding TAT-SMNs were generated using standard DNA recombination techniques using inserts generated by polymerase chain reaction (PCR). The plasmids expressing TAT-GFP in mammalian cells are derived from pJB100, which is the result of inserting sequences encoding enhanced green fluorescent protein (eGFP) with a 6xHis tag and a streptavidin tag on the C terminus into the commercial plasmid pcDNA3.1 (Invitrogen, Carlsbad, CA) and is under the control of a cytomegalovirus (CMV) promoter. Amplicons encoding three variants of the TAT PTD were inserted at the N terminus of the eGFP between an NheI restriction site and an AgeI restriction site. Constructs which encode a secretory peptide had an amplicon inserted either at the N terminus of the eGFP or at the N terminus of the TAT PTD (at the NheI site), if one was present. TAT-GFP constructs for the bacterial system feature the same sequences of interest as their mammalian counterparts but inserted into the commercial plasmid pET21-d (Millipore, Billerica, MA) and expression is controlled by a T7 promoter. Plasmids encoding TAT-SMN are derived from pCI-neo (Promega, Fitchburg, WI). TAT-SMN amplicons were inserted between an NheI site and an MluI site, and the SP sequence, if present, was inserted at the N terminus of the TAT PTD or at the N terminus of SMN if no TAT PTD is present. A set of GFP-tagged SMN constructs was generated by cloning a 1.6 kb sequence encoding a CMV promoter-controlled SMN into the eGFP-containing plasmid pJB100, generating an SMN-GFP fusion. An SpeI/BamHI fragment was excised from the N-terminus of the SMN-GFP construct and replaced with a fragment encoding SP, SP-TAT3, or SP-TATκ to generate secretable TAT-SMN-GFP constructs. The SMN-GFP plasmids also encoded a non-secreted RFP which was separate from

the fusion protein and controlled by a separate CMV promoter. All constructs were confirmed through sequencing (Stemcore, OHRI). Important constructs are highlighted in Table 2.1.

## 2.2: Mammalian cell culture methods

### 2.2.1: Cell culture

293 (human embryonic kidney) cells which express the adenoviral E1 proteins were maintained in minimal essential media (MEM, Gibco, Carslbad, CA) supplemented with 10% fetal bovine serum (FBS, Sigma-Aldrich), 1% Glutamax (Gibco), and 1% anti-biotic anti-mycotic (Gibco) in a 5% $CO_2$ environment at 37ºC in a Sanyo incubator (Sanyo, Wood Dale, IL). A549 cells (human lung epithelial carcinoma, American Type Culture Collection CCL-185) were maintained using the same media and conditions as the 293 cells.

### 2.2.2: Expression of TAT-GFPs in mammalian cells

Five micrograms of each TAT-GFP plasmid containing a CMV promoter was added to a 15 mL conical tube containing 300 µL of serum-free media with 10 µL of Superfect transfection reagent (Qiagen, Germantown, MD) for 10 minutes. Following this incubation, 1.8 mL of serum-free media was added to each tube to terminate the complex formation reaction. Thirty-five millimetre plates confluent with 293 cells ($1.2 \times 10^6$ cells) were washed with phosphate-buffered saline (PBS) prior to the addition of the transfection mixtures. The cells were incubated for 3 hours at 37ºC in the transfection mixtures before this media was removed and replaced with fresh 10% FBS media and incubated at 37ºC overnight. Twenty-four hours post-transfection the cells were visualized using fluorescence microscopy (Zeiss Axiovert 200M, Zeiss, Jena, Germany).

**Table 2.1:** List of DNA constructs used in the present work. Intermediate constructs or constructs which were ultimately not used are excluded.

| Construct Name | System | Parental Plasmid | Inserts |
|---|---|---|---|
| pJB100 | mammalian | pcDNA3.1 | GFP |
| pJB101 | " | " | TAT-GFP |
| pJB102 | " | " | TAT3-GFP |
| pJB103 | " | " | TATκ-GFP |
| pJB104 | " | " | SP-GFP |
| pJB105 | bacterial | pET21-d | GFP |
| pJB106 | " | " | TAT-GFP |
| pJB107 | " | " | TAT3-GFP |
| pJB108 | " | " | TATκ-GFP |
| pJB109 | mammalian | pcDNA3.1 | SP-TAT-GFP |
| pJB110 | " | " | SP-TAT3-GFP |
| pJB111 | " | " | SP-TATκ-GFP |
| pJB121 | " | pCI-neo | SP-SMN |
| pJB122 | " | " | SP-TAT3-SMN |
| pJB123 | " | " | SP-TATκ-SMN |
| pJB124 | " | pcDNA3.1 | SMN-GFP, RFP |
| pJB125 | " | pCI-neo | SP-SMN-GFP, RFP |
| pJB126 | " | " | SP-TAT3-SMN-GFP, RFP |
| pJB127 | " | " | SP-TATκ-SMN-GFP, RFP |

The media was then removed and the cells were washed with PBS prior to being collected in 200 µL of 2x Laemmli buffer (8% Tris-HCl pH 6.8, 25% glycerol, 5% β-mercaptoethanol, 2% SDS, 0.01% bromophenol blue).

### 2.2.3: Transduction of mammalian TAT-GFPs

293 cells which had been transfected with constructs encoding mammalian TAT-GFPs were collected in 1 mL of PBS and frozen at -20ºC. The following day the samples were thawed and centrifuged at 16,000xg for 5 minutes. The supernatant was collected and applied to A549 cells which were incubated at 37ºC for 4 hours. After incubation, the supernatant was removed and the cells were washed with PBS, then with trypsin to remove any GFP or TAT-GFP that had adhered to cells but not transduced the cells. Media containing 10% FBS was added to the cells immediately after removing the trypsin and cells were visualized by fluorescence microscopy. The media was then removed and the cells were washed once more with PBS before being collected in Laemmli buffer.

### 2.2.4: Cell transfer using TAT-SMN-GFPs

293 cells were transfected with 5 µg of constructs encoding an SP-TAT-SMN-GFP fusion protein and a separate RFP. The day after transfection, the expression of the fusion protein was verified using fluorescence microscopy and the cells and/or media was collected and applied to a second plate containing untransfected 293 cells. For cell transfer experiments, 10% of the transfected cells were added to confluent plates of untransfected cells. In media transfer experiments, all of the media (2 mL) from the transfected cells was applied to the untransfected cells. In both cases the cells were incubated overnight at 37ºC and visualized by fluorescence

microscopy 24 hours later.

### 2.2.5: Recovery of secreted proteins from media

All media from each plate (2 mL) was collected 24 hours after transfection or 18 hours following infection. The media was centrifuged at 16,000xg for 5 minutes to pellet any cell debris. The supernatant was then passed through a 0.45 μm filter (Corning) using a syringe. One millilitre of the filtrate was treated with 250 μL of 100% w/v trichloroacetic acid (TCA, Sigma-Aldrich) and incubated on ice for 30 minutes. The resulting suspension was centrifuged at 16,000xg for 5 minutes, after which the supernatant was discarded and the pellet washed with 200 μL of 100% ethanol. The samples were centrifuged again at 16,000xg for 5 minutes. The supernatant was removed and the precipitates were resuspended in 100 μL of 2x Laemmli buffer.

## 2.3: Bacterial methods

### 2.3.1: Bacterial culture

*Escherichia coli* of the DH5α strain were transformed with ligated constructs to generate plasmids for transfection into mammalian cells. The bacteria were transformed with a plasmid containing an ampicillin resistance gene and incubated overnight at 37ºC on agar plates (Thermo-Fisher Scientific, Waltham, MA) containing 50 μg/mL ampicillin. Colonies were picked from the plate on the following day and incubated overnight at 37ºC in Luria broth (Thermo-Fisher) with constant agitation. One millilitre of each bacterial suspension was used to generate plasmid minipreps (Sigma GenElute Kit, Sigma-Aldrich. St. Louis, MO), which were subsequently subjected to restriction digest screening. Colonies whose minipreps yielded the expected

restriction digest profile were used as inoculum to generate large-scale preparations of their plasmids. A second strain of *E. coli,* BL21, was used to generate large-scale protein preps. These bacteria were transformed with a TAT-GFP plasmid and incubated at 37 ºC overnight on agar plates containing ampicillin. Colonies were picked from each plate the following day and added to 200 mL of LB amp+. On the third day, 5 mL of the 200 mL culture was added to 45 mL of LB amp+ along with 50 µL of isopropyl β-D-1-thiogalactopyranoside (IPTG, Promega, Madison, WI) to induce protein expression. The resulting suspension was incubated for 6 hours at 37ºC with agitation. The suspension was then centrifuged at 8000xg at 4ºC for 30 minutes. The supernatant was discarded and the pellet was resuspended in 6.7 mL of lysis/binding buffer (50 mM $NaH_2PO_4$, 300 mM NaCl, 10 mM imidazole, pH 8) to which 700 µL of lysozyme (10 mg/mL, Sigma-Aldrich) was added. The bacterial suspensions were frozen at -20ºC until purification.

### 2.3.2: Purification of bacterial TAT-GFPs

Lysates of IPTG-induced BL21 cultures containing TAT-GFPs were thawed and centrifuged for 30 minutes at 8,000xg at 4ºC. The supernatants were collected and passed through a 0.45 µm syringe filter (Corning, Tewksbury, MA) into a 15 mL conical tube. These filtrates were applied to a Ni-NTA Superflow column (Qiagen) and purified according to the manufacturer's instructions. A small amount of the filtrates was retained for use as an input sample while assessing the effectiveness of the columns. Flow-through, two washes, and the final eluate were collected for analysis. Once the presence of the desired protein was confirmed in the eluate through Western blotting, the eluates were dialyzed against 10 mM Tris-HCL (pH 8) overnight, with one change of the Tris-HCL occurring 4-6 hours into the dialysis. The amount of protein

present in the dialyzed eluate was determined by loading the eluates onto a polyacrylamide gel alongside a range of BSA standards (0.5 - 0.01 mg/mL) and performing electrophoresis. The gel was then stained with Coomassie Blue dye (50% methanol, 10% acetic acid, 0.05% bromophenol blue in $dH_2O$) for 30 minutes and washed with destain solution (50% methanol, 10% acetic acid in $dH_2O$) multiple times before destaining overnight at 4ºC. The stained gel was placed between two acetate sheets and an image was obtained using an EPSON GT-1500 scanner (EPSON, Markham, ON).

### 2.3.3: Transduction of bacterial TAT-GFPs

The relative amount of protein present in the dialyzed eluates was determined via Western blotting. Two hundred microlitres of eluate (or an appropriate dilution of eluate in PBS) was applied to A549 cells in a 24-well plate (Corning). The cells were incubated for 4 hours at 37ºC, washed with PBS, then with trypsin. After the trypsin wash, 10% FBS media was added to the cells and they were visualized under a fluorescence microscope. The media was removed and the cells were washed once more with PBS prior to collection in 100 µL of Laemmli buffer.

## 2.4: Adenoviral methods

### 2.4.1: Adenovirus production

A 2.0 kb SpeI/NotI fragment from pJB118, pJB119, or pJB120 was cloned into the pRP2645 Ad left-end shuttle plasmid [144], generating pJB128, pJB129, pJB130. These shuttle plasmids were then recombined into pRP2014, an Ad genomic plasmid [144], using bacterial

RecA-mediated recombination [145], generating pJB131, 132 and 133. These three plasmids were transfected into 293 cells and rescued into viruses using standard techniques [146].

### 2.4.2: Infections

A549 cells were seeded onto 35 mm plates and grown to confluency. Adenoviruses were applied at a multiplicity of infection (MOI) of 100 or 10 diluted in PBS to a final volume of 100 µL and the cells were incubated at 37ºC for 1 hour with rocking once every 15 minutes. Following this incubation, 2 mL of 10% FBS media was added to each plate and the cells were incubated for an additional 17 hours at 37ºC.

### 2.4.3: Treatment with conditioned media

Media (2 mL) was collected from plates 18 hours after infection with viruses encoding SP-TAT-SMNs and centrifuged at 16,000xg for 5 minutes. The supernatant was passed through a 0.20 µm syringe filter (Corning) and then applied to a 100 kDa size exclusion column (Amicon Ultra, Millipore) and centrifuged at 16,000xg for 10 minutes to exclude virus particles. The filtrate was then applied to A549 cells which were subsequently incubated for 2 hours at 37ºC. Following incubation, the conditioned media was removed and the cells were washed with PBS, trypsin, 10% FBS media, and PBS again prior to being harvested in 100 µL of 2x Laemmli buffer.

## 2.5: Western blot

Following separation of proteins by 12% SDS-PAGE, the gels were transferred to an Immobilon membrane (Millipore) using a semi-dry transfer apparatus (Bio-Rad, Hercules, CA). Following transfer, the membrane was incubated overnight at 4ºC or for 1 hour at RT in blocking

solution (5% skim milk in TBST 20mM: Tris-HCl pH 7.6, 137 mM NaCl, and 0.1% Tween 20). Next, the appropriate primary antibody was added to the blocking solution and the membrane was incubated for either 1 hour at RT with constant agitation or overnight at 4ºC (Table 2.2). The membranes were washed with TBST three times for 5 minutes each before blocking solution was added again containing a secondary antibody conjugated to horseradish peroxidase (HRP) which targeted the species of the primary antibody. Membranes were incubated in secondary antibody for 1 hour at RT with constant agitation. The membranes were rinsed again three times in TBST for 5 minutes each and then treated for 5 minutes with ECL substrate (Pierce ECL Western Blotting Substrate, Thermo-Fisher), which acts as the substrate for the activity of HRP. The resulting chemiluminescent reaction was detected using X-ray film. The presence of a band on the X-ray film thereby indicates the presence of the protein of interest on the membrane.

**Table 2.2:** List of antibodies used in the present work. Dilution of secondary antibodies varied by experiment.

| Antibody | Species | Dilution | Source |
|---|---|---|---|
| α-GFP | rabbit | 1:5000 | Life Technologies, Eugene, OR |
| α-tubulin | mouse | 1:10000 | Millipore (Calbiochem) |
| α-SMN | mouse | 1:5000 | BD Biosciences, Franklin Lakes, NJ |
| α-FLAG | mouse | 1:5000 | Rockland, Gilbertsville, PA |
| α-mouse (HRP) | goat | 1:10000 or 1:5000 | Bio-Rad |
| α-rabbit (HRP) | goat | 1:10000 or 1:5000 | Bio-Rad |

# Chapter 3 – Results

## 3.1: Transient transfection in mammalian cells

### 3.1.1: Generation of fusion proteins

To facilitate comparison of the relative transduction capability of three TAT PTD variants, eGFP with a 6x histidine tag and a streptavidin tag at the carboxy terminus was inserted into the commercial plasmid pcDNA3.1. One of three TAT PTD variants was inserted in frame at the amino terminus of the GFP: the native sequence of the protein transduction domain [139], denoted as TAT; a mutant featuring a reduction in basic amino acid residues denoted as TAT3 which was previously found to exhibit superior transduction capability [147]; and a mutant similar to TAT3 designed to resist cleavage by furin, denoted as TATκ [143]. The amino acid sequence of TAT3 also renders it resistant to furin cleavage. To assess the viability of a secreted therapeutic protein, a secretory peptide derived from the V-J2-C region of murine Ig κ-chain was inserted into the plasmids at the N-terminus of the TAT PTD or the GFP if no PTD was present. A schematic representation of these constructs is found in Figure 3.1A.

To investigate the performance of the TAT PTDs and the SP in an SMN fusion, SMN with an N-terminal FLAG tag was first inserted into the commercial plasmid pCI-neo. One of the three TAT-PTD variants was inserted at the N terminus of SMN and the SP, if present, was inserted at the N terminus of the TAT PTD or, if no TAT PTD was present, at the N terminus of SMN. Another set of SMN constructs was generated for visualization of fusion SMNs by fluorescence microscopy. These constructs featured a GFP fused in frame to the carboxy terminus of SMN in

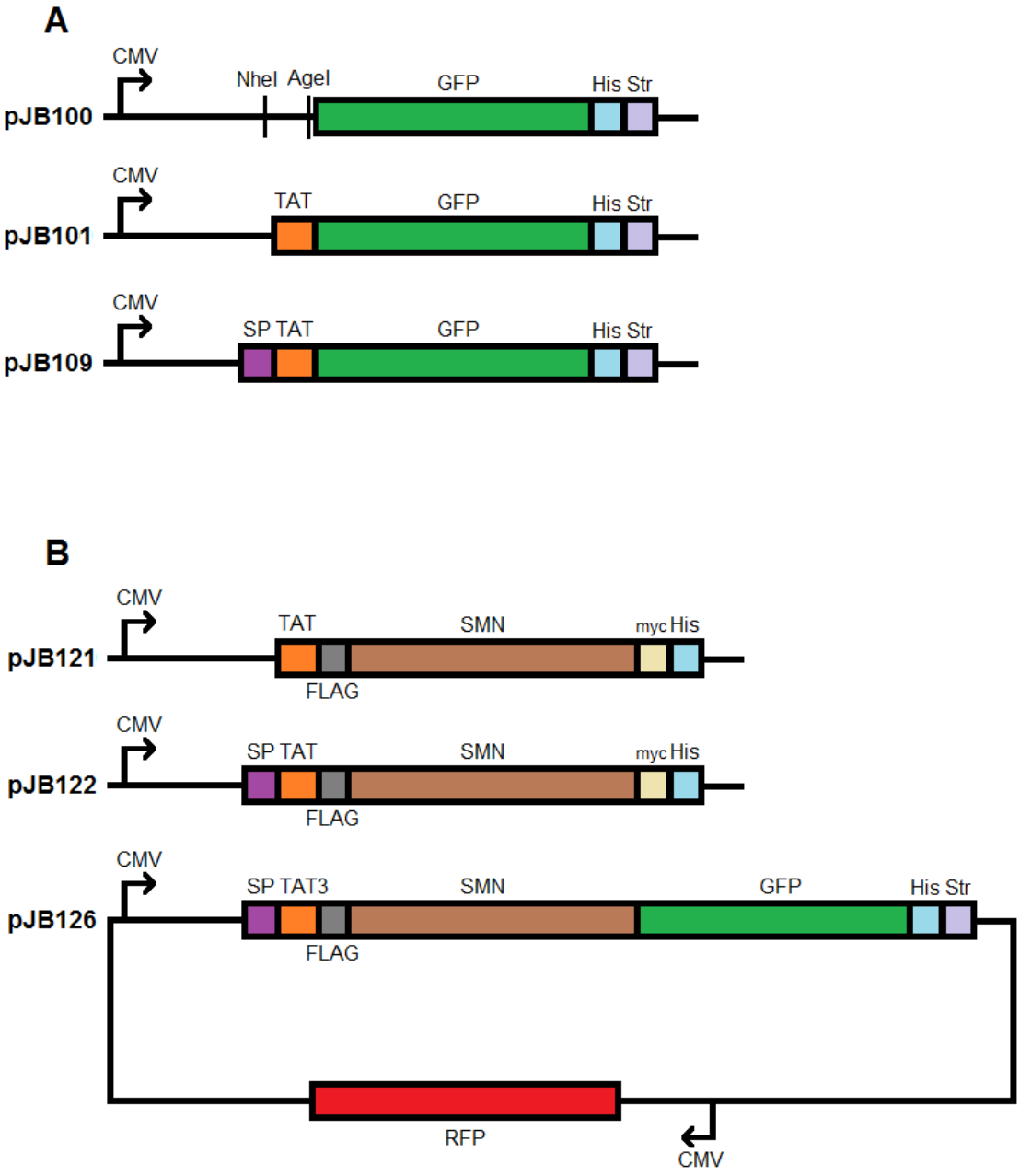
A
CMV
NheI AgeI
GFP
His Str
pJB100
CMV
TAT
GFP
His Str
pJB101
CMV
SP TAT
GFP
His Str
pJB109
B
CMV
TAT
SMN
myc His
FLAG
pJB121
CMV
SP TAT
SMN
myc His
FLAG
pJB122
CMV
SP TAT3
SMN
GFP
His Str
FLAG
pJB126
RFP
CMV

**Figure 3.1:** Schematic representations of constructs for transient transfection. A representative construct from each category is presented here. Panel A: All GFP constructs feature a motif of six repeated histidine residues to allow for $Ni^{2+}$ column purification and a streptavidin tag for further purification. Panel B: SMN constructs feature a FLAG tag for detection and differentiation from endogenous SMN by immunoblot.

addition to the amino terminus modifications found in the other SMN constructs. The SMN-GFP constructs also featured an RFP on a separate CMV promoter to allow differentiation between cells which express the plasmid and cells which have received protein via secretion and transduction. Schematics of the SMN constructs are found in Figure 3.1B.

### 3.1.2: Expression of TAT-GFPs in mammalian cells

Once the constructs had been generated, the expression capability of the mammalian TAT-GFP constructs was assessed *in vitro*. 293 cells were seeded onto 60 mm plates and grown to confluency. The cells were transfected with 5 μg of a plasmid encoding GFP, TAT-GFP, TAT3-GFP, TATκ-GFP, SP-GFP, SP-TAT-GFP, SP-TAT3-GFP, or SP-TATκ-GFP and incubated for 3 hours at 37ºC. Following this incubation, the transfection media was removed and replaced with 10% FBS MEM. Cells were lysed and collected in Laemmli buffer 24 hours post-transfection and subjected to SDS-PAGE and Western blotting (Figure 3.2). The signals generated when the blot was probed with an α-GFP antibody suggest that all of the constructs are expressing, but that there is variation in the degree to which each is expressed. TAT-GFP expresses less strongly compared to its TAT3 and TATκ counterparts, and all three SP-TAT-GFPs express relatively weakly, though they display a similar degree of expression to one another. The α-tubulin controls indicate that an approximately equal amount of each lysate was applied to the gel, so the variations in GFP signal strength may be due to differences in transfection efficiency or protein stability. Two bands are present in the lanes corresponding to all of the fusions which contain a TAT PTD. This is likely caused by the presence of the original start codon in the GFP sequence: translation initiation at the downstream, native ATG would result in unmodified GFP being expressed in addition to the fusion protein. The presence of a TAT PTD caused a shift in band size of approximately 5 kDa for

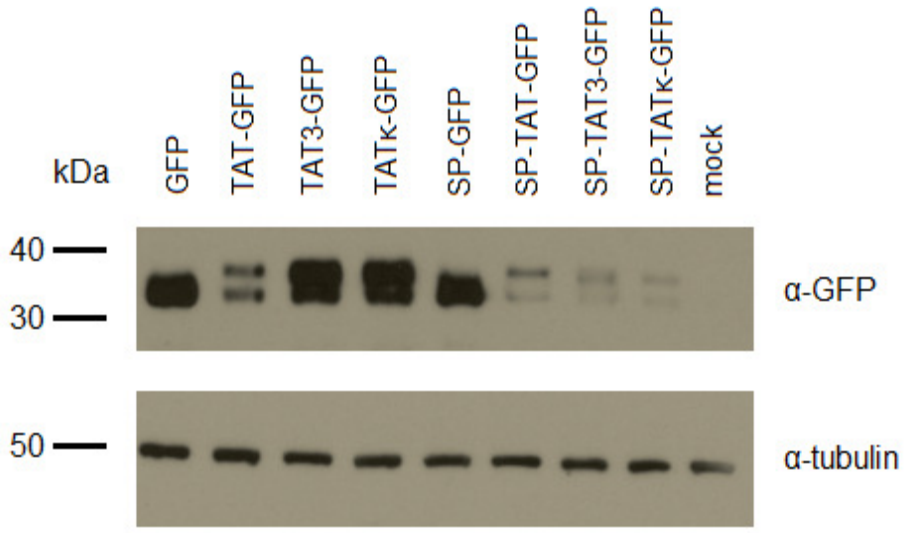
kDa
GFP
TAT-GFP
TAT3-GFP
TATκ-GFP
SP-GFP
SP-TAT-GFP
SP-TAT3-GFP
SP-TATκ-GFP
mock
40
30
50
α-GFP
α-tubulin

**Figure 3.2:** Expression of mammalian TAT-GFP constructs. 293 cells were transfected with 5 μg of a GFP construct (or 5 μL of $dH_2O$ in the mock transfection) for 3 hours. Media was changed and the cells were incubated overnight. Cell lysates were collected and subjected to electrophoresis on a 12% polyacrylamide gel. This Western blot suggests that all constructs were successfully expressed but that the constructs varied in regard to protein yield. The tubulin control suggests that the variation in GFP signal strength was not caused by uneven loading of cell lysates. In a second iteration of this experiment the variability of GFP protein yield appeared to be less extreme.

the fusion protein in which one was present. Thus, the TAT-GFP constructs expressed well in mammalian cells, though unmodified GFP protein was also expressed.

### 3.1.3: Transduction of TAT-GFPs *in vitro*

Transduction capability of the mammalian TAT-GFPs was assessed by applying lysate from cells transfected with TAT-GFP constructs to new, untransfected 293 cells and incubating for 4 hours. Lysates from the second population of cells were analyzed by immunoblotting (Fig. 3.3). GFP was detected in the cells treated with GFP only in the absence of a TAT PTD, which suggests that GFP alone may be crossing cell membranes in the treated population, or the trypsin wash is not eliminating all GFP. The signal observed in Fig. 3.3 in the first four lanes is the expected size of a normal GFP, not a TAT-GFP fusion protein, which suggests that the TAT PTD does not confer an enhancement in transduction capability. A preliminary experiment suggested that the TAT PTD did in fact enhance transduction (not shown), but this finding proved inconsistent using this experimental approach. The methods used for this experiment were designed to allow us to compare transduction capability of the TAT PTD variants independent of secretion, but this method yields only a small amount of TAT-GFP, and it is difficult to normalize the amount of protein with which each plate of recipient cells is treated. These results indicated that we needed to generate a larger amount of protein in order to compare the capabilities of the three TAT variants.

### 3.1.4: Secretion of SP-TAT-GFPs *in vitro*

Though the mammalian system proved challenging for the assessment of transduction

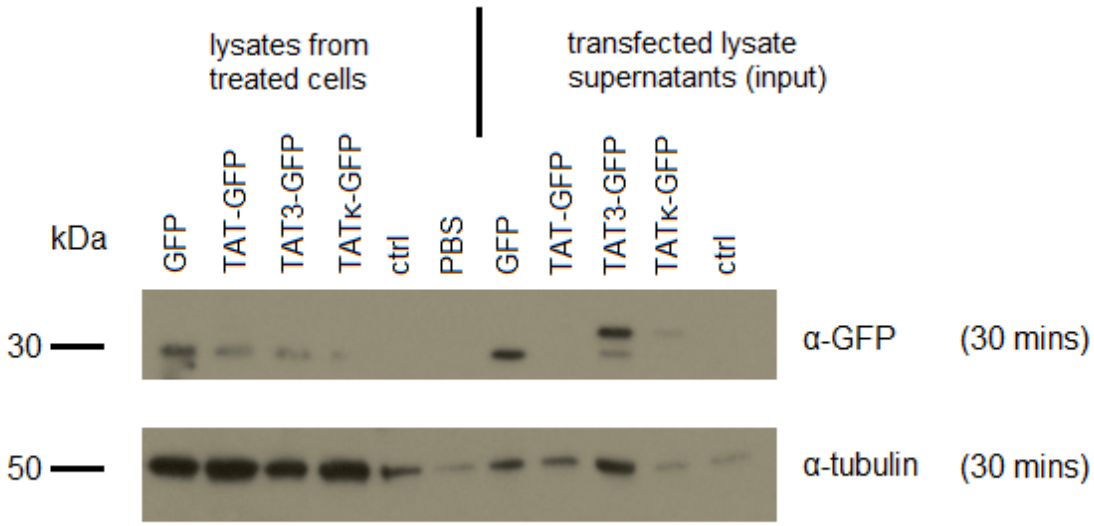
lysates from
treated cells
transfected lysate
supernatants (input)
kDa
GFP
TAT-GFP
TAT3-GFP
TATκ-GFP
ctrl
PBS
GFP
TAT-GFP
TAT3-GFP
TATκ-GFP
ctrl
30
α-GFP
(30 mins)
50
α-tubulin
(30 mins)

**Figure 3.3:** Transduction of mammalian TAT-GFP proteins. 293 cells were transfected with 5 μg of DNA constructs encoding GFP or a TAT-GFP. The following day the transfected cells were lysed using a freeze-thaw cycle and the lysates were centrifuged. Supernatants were applied to new 293 cells for 4 hours. The lysate-treated 293 cells were washed with PBS and then with trypsin to remove GFP that had adhered to the cell surface but had not transduced the cells. MEM containing 10% FBS was added to quench the activity of trpysin and the cells were rinsed once more with PBS. The cells were then lysed in Laemmli buffer and subjected to electrophoresis and immunoblotting.

capability, we were able to observe secretion of the fusion proteins *in vitro*. Plasmids encoding SP-GFP or an SP-TAT-GFP were transfected into 293 cells in 60 mm dishes, which were incubated at 37ºC overnight. Following this incubation the media (2 mL) was removed from each plate and filtered, and 1 mL from each media sample was subjected to protein precipitation using TCA. The cells were washed with PBS and then collected in Laemmli buffer. Resuspended protein precipitates were subjected to SDS-PAGE along with the cell lysates and the presence of GFP or TAT-GFP was detected using an α-GFP Western blot. The signals in Figure 3.4 suggest that the SP-GFP and SP-TAT3-GFP are being secreted effectively, and TATκ-GFP is likely secreted to a lesser extent. No GFP signal is present in the TAT-GFP media precipitate lane, suggesting that the SP is ineffective when fused to the native TAT PTD. A faint signal in the control GFP lane (in the absence of an SP) suggests that there may be some leakage of unmodified GFP. The media precipitates were also probed with an α-tubulin antibody to determine whether GFP release into media was caused by cell death. The absence of tubulin signals in these lanes suggests that cell death was not the mechanism by which the GFPs escaped the cell. Ultimately we were able to observe secretion of the SP-fused proteins *in vitro* for most of the GFP constructs we transfected into mammalian cells.

### 3.1.5: Secretion and transduction of SMN-GFPs

In order to assess secretion and subsequent uptake of secreted TAT-SMN, we generated constructs which encoded SMN-GFP fused to SP and/or a TAT PTD to allow for visualization of our fusion SMNs by fluorescence microscopy. The constructs also encoded RFP under a separate promoter so that we could visualize cells that were expressing the plasmid and compare them with those that contained the fusion proteins. Cells in which our GFP-tagged proteins were detected

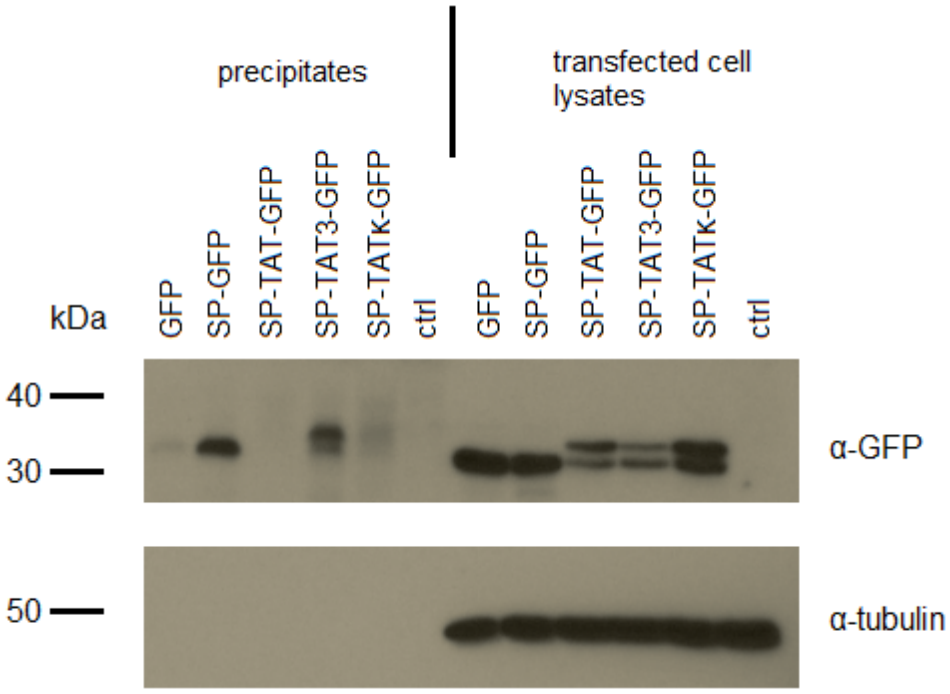
precipitates
transfected cell lysates
kDa
GFP
SP-GFP
SP-TAT-GFP
SP-TAT3-GFP
SP-TATκ-GFP
ctrl
GFP
SP-GFP
SP-TAT-GFP
SP-TAT3-GFP
SP-TATκ-GFP
ctrl
40
30
α-GFP
50
α-tubulin

**Figure 3.4:** Secretion of SP-GFP proteins. 293 cells were transfected with plasmids encoding SP-GFP or an SP-TAT-GFP. Protein was precipitated from the media using TCA and the resuspended precipitates were subjected to SDS-PAGE with lysates of the transfected cells. The Western blot was probed α-GFP to detect the proteins of interest in the precipitates and lysates, then α-tubulin to act as a loading control for the lysates and to assess the contribution of cell death to the release of GFP into media.

but no RFP was being expressed would indicate that the fusion proteins are being secreted by transfected cells and are subsequently transducing untransfected cells. A primary population of 293 cells was transfected with 5 μg of a plasmid encoding SMN-GFP, SP-SMN-GFP, SP-TAT3-SMN-GFP, or SP-TATκ-GFP and incubated overnight at 37ºC. Following incubation, $1/10^{th}$ of the transfected cells were transferred to a secondary population of untransfected 293s and incubated for 24 hours at 37ºC. A rare example of a cell displaying green fluorescence but not red fluorescence is shown in Figure 3.5. In most cases any cells in which the SMN-GFP was found also expressed the RFP found on the plasmid. In an attempt to eliminate the effect of cell division or miscalls regarding the absence of RFP we performed similar experiments in which only the media from transfected cells were transferred, but these yielded no positive results. Taken together, these data suggest that this approach lacks the sensitivity necessary to accurately evaluate secretion and uptake of SMN.

### 3.1.6: Conclusion

The data presented in Figure 3.3 indicates that a greater amount of protein is needed to compare the transduction efficiency of the three TAT PTD variants. Further, the results of Figure 3.5 suggest that transient transfection of these constructs into mammalian cells does not generate enough protein to allow evaluation of secretion and uptake of the SMN fusions. Therefore, we moved into a bacterial system to generate large amounts of TAT fusion proteins (Section 3.2 of the present work) and developed an adenovirus-based system to evaluate secretion (Section 3.3).

A

B

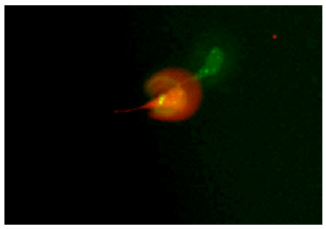

C

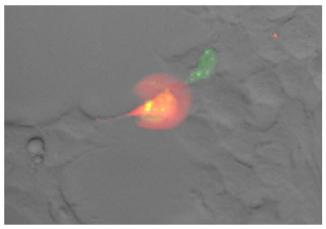

**Figure 3.5:** Secretion and transduction of SMN-GFP proteins. A primary population of 293s was transfected with constructs encoding SMN-GFP, SP-SMN-GFP, SP-TAT3-SMN-GFP, or SP-TATκ-GFP and incubated overnight. The transfected cells were diluted 1:10 and $1/10^{th}$ of the solution was added to a secondary population of 293 cells. The combined population was visualized by fluorescence microscopy after 24 hours of co-culturing. Red fluorescence indicates the presence of the transfected construct within the cell. Green fluorescence indicates the presence of the fusion protein of interest. In this image an untransfected cell containing fusion protein was found adjacent to a cell which had been had been transfected with the SP-TAT3-SMN-GFP construct. Panel A: Cells photographed at 500 ms exposure colourized by software. Panel B: Image from Panel A enhanced by software to highlight green fluorescence. Panel C: Overlay of fluorescent signals on cells photographed using a halogen lamp.

### 3.2: TAT-GFP production in *E. coli*

#### 3.2.1.: Bacterial constructs

To address the problem of low TAT-GFP yield in the mammalian system, we generated constructs encoding our TAT-GFPs for expression in *E. coli.* These constructs were derived from the commerical plasmid pET21-d and contain GFP with a 6x histidine tag and a streptavidin tag, with or without TAT PTD fused to the N terminus of GFP (Figure 3.6).

#### 3.2.2: Production of bacterial TAT-GFPs

To generate large preparations of the three TAT-GFPs (and a control GFP), we first transformed the constructs into BL21 bacteria which were subjected to ampicillin selection. Ampicillin-resistant colonies were picked and used to generate 200 mL cultures, from which 5 mL was added to 45 mL of LB amp+ in the presence of 50 μL of IPTG. Inducing the bacteria in this manner during an exponential growth phase results in the production of TAT-GFP, which is shown in Figure 3.7A. This panel compares column eluates and inputs of induced (+) and non-induced cultures containing the TATκ-GFP plasmid alongside parental plasmid controls. No GFP is observed in the lanes corresponding to the non-induced TATκ-GFP culture or either of the control plasmid cultures regardless of induction. GFP is present in the induced TATκ-GFP culture only. The induced cultures were lysed and centrifuged, and the supernatant was applied to a $Ni^{2+}$ gravity flow column. Figure 3.7B shows a representative example of input, flowthrough, wash, and eluate fractions from these columns, in which a large amount of TAT3-GFP is recovered, though the additional band of lower molecular weight indicates that a significant amount of regular GFP (i.e. no TAT PTD) was also present in the eluate. The eluates from the nickel columns

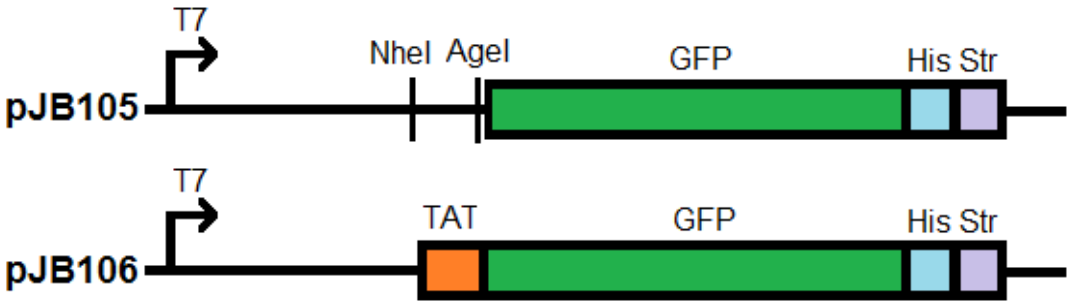
T7
NheI
AgeI
GFP
His Str
pJB105
T7
TAT
GFP
His Str
pJB106

**Figure 3.6:** Schematic representation of bacterial TAT-GFP constructs.

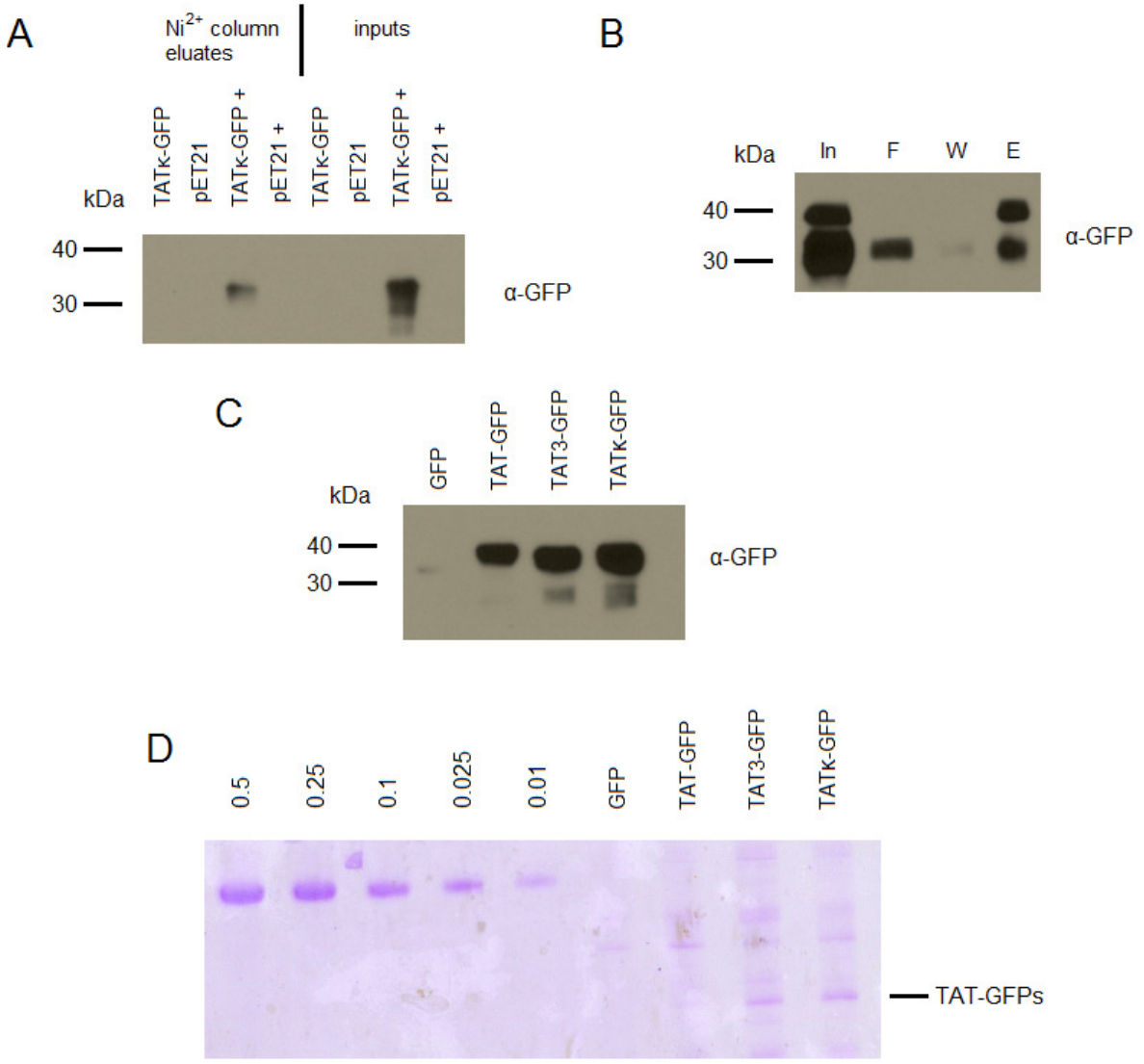
A
Ni2+ column eluates
inputs
TATκ-GFP
pET21
TATκ-GFP +
pET21 +
TATκ-GFP
pET21
TATκ-GFP +
pET21 +
kDa
40
30
α-GFP
B
kDa
In
F
W
E
40
30
α-GFP
C
GFP
TAT-GFP
TAT3-GFP
TATκ-GFP
kDa
40
30
α-GFP
D
0.5
0.25
0.1
0.025
0.01
GFP
TAT-GFP
TAT3-GFP
TATκ-GFP
TAT-GFPs

**Fig. 3.7:** Production of TAT-GFP proteins using BL21 *E. coli.* Bacteria were transformed with plasmids encoding GFP or TAT-GFPs and subjected to ampicillin selection. Transformed cultures were induced with 1 mM IPTG during the exponential growth phase and collected after 6-8 hours. Induced cultures were lysed and centrifuged and the supernatant was applied to a gravity flow nickel column. Panel A: Induced cultures (indicated by +) yielded signal on immunoblots using an α-GFP antibody, and non-induced cultures did not. Panel B: Immunoblots of the input (In), flowthrough (F), wash (W), and eluate (E) fractions show that a significant amount of TAT-GFP is recovered in the eluate, but that non-TAT tagged GFP is still present. Panel C: Following dialysis, the amount of protein present in each of the three TAT-GFP eluates is comparable to the others, but the control GFP eluate consistently contained less protein. Panel D: Performing SDS-PAGE using dialyzed eluates and BSA standards (0.5 – 0.01 mg/mL) and staining with Coomassie blue dye allowed for quantification of the GFP and TAT-GFPs in the dialyzed eluates. BSA standards and dialyzed eluates were loaded in equal volumes (15 μL) to allow direct comparison of protein concentration.

were dialyzed prior to their use in GFP transduction experiments. A comparison of the relative amount of protein in each dialyzed eluate is found in Figure 3.7C, alongside the dialyzed eluate of a culture transformed with a control GFP. The amount of protein in each of the three TAT-GFP eluates is comparable to the others, but yield was consistently lower for the control GFP. For transduction experiments, the amount of protein applied had to be normalized, so we quantified the dialyzed eluates using a range of BSA standards in a Coomassie blue stain (Figure 3.7D). The amount of protein observed in each eluate varied each time these proteins were prepared, however in this instance the concentrations were estimated to be $1x10^{-4}$ mg/mL for GFP, $1x10^{-3}$ mg/mL for TAT-GFP, and 0.01 mg / mL for TAT3-GFP and TATκ-GFP.

### 3.2.3: Transduction of bacterial TAT-GFPs

Dialyzed eluates were normalized by diluting eluates with higher TAT-GFP concentration in PBS to generate treatment aliquots that were approximately equivalent in concentration. A549 cells were seeded on a 24-well plate and grown to confluency. The cells were treated with 200 μL of GFP or TAT-GFP eluate for 4 hours at 37ºC. A control well was treated with PBS. After 4 hours the protein treatments were removed and the cells were washed with PBS, and then with trypsin to remove attached proteins that had not been internalized. MEM containing 10% FBS was added to neutralize the trypsin and the cells were visualized by fluorescence microscopy. Figure 3.8 shows that TAT3-GFP and TATκ-GFP appear to cross cell membranes more readily than TAT-GFP, when the relative concentration of each TAT-GFP is the same, however all three appear to show enhancement in membrane transduction compared to the control GFP. Some faint fluorescence can be observed in the image for the control GFP, which may be caused by GFP adhering to cellular debris or this may indicate that the trypsin wash is not completely effective in

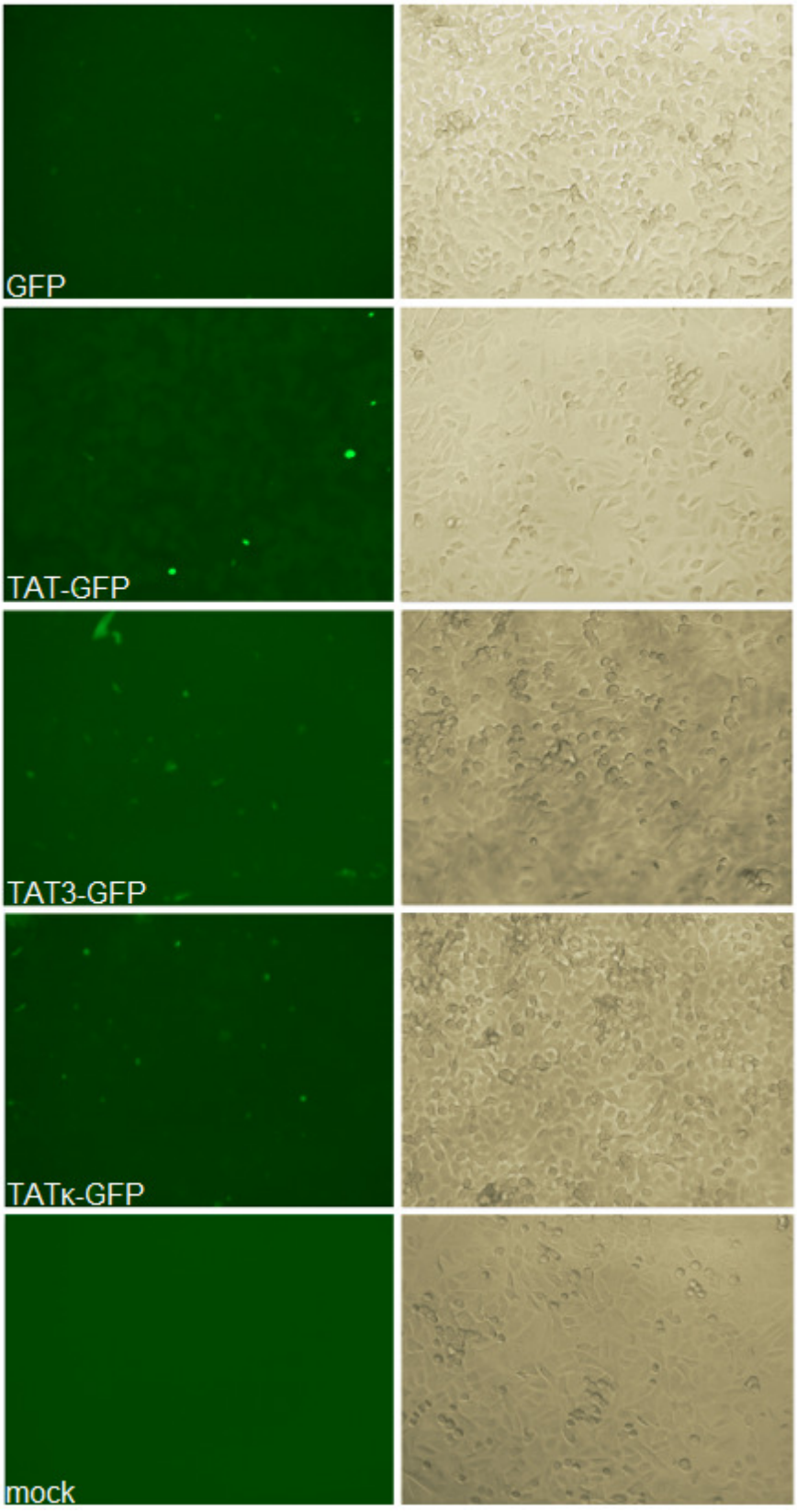
GFP
TAT-GFP
TAT3-GFP
TATκ-GFP
mock

**Figure 3.8:** Visualization of bacterial TAT-GFP transduction. A549 cells were treated with dilutions of the dialyzed protein samples for 4 hours and then visualized by fluorescence microscopy using a 20X objective. Raw green fluorescence images were taken with a camera (500 ms exposure) and coloured using software, shown alongside phase contrast images of the same visual field.

removing GFP that has adhered to the surface of cells. After microscope images were taken, the media was removed and the cells were washed once more with PBS before being lysed in Laemmli buffer. Cell lysates were subjected to SDS-PAGE and Western blotting alongside dialyzed protein inputs (Figure 3.9). The inputs appear to separate differently from the lysates and the protein ladder in Figure 3.9, possibly because the inputs are purified protein in 1mM Tris-HCL rather than cell lysates collected in 2x Laemmli buffer. However, the bands in the input GFP lane in panel A are not the expected size for GFP. TAT-GFP and TAT3-GFP consistently yielded signals on Western blots probed with α-GFP. TATκ-GFP yielded signal in some iterations of this experiment (Figure 3.9A), but not in others (Figure 3.9B), suggesting that transduction of this protein is inconsistent. The lower band representing GFP without a TAT PTD which is often present in treated cell lysates was not present in the TAT3-GFP input or treated cell lysate, suggesting that this protein might have less contamination by unmodified GFP compared to the other TAT PTDs.

### 3.2.4: Conclusion:

The data suggests that all three TAT variants facilitate transduction; however, the apparent inability of TAT-GFP to be secreted presented in Figure 3.4 suggests that the native TAT PTD is not appropriate for our secreted therapeutic protein. The inconsistent transduction capability demonstrated by TATκ in Figure 3.8 raises questions about its reliability in therapeutic use. Therefore, TAT3 appears to be the best option for our purposes.

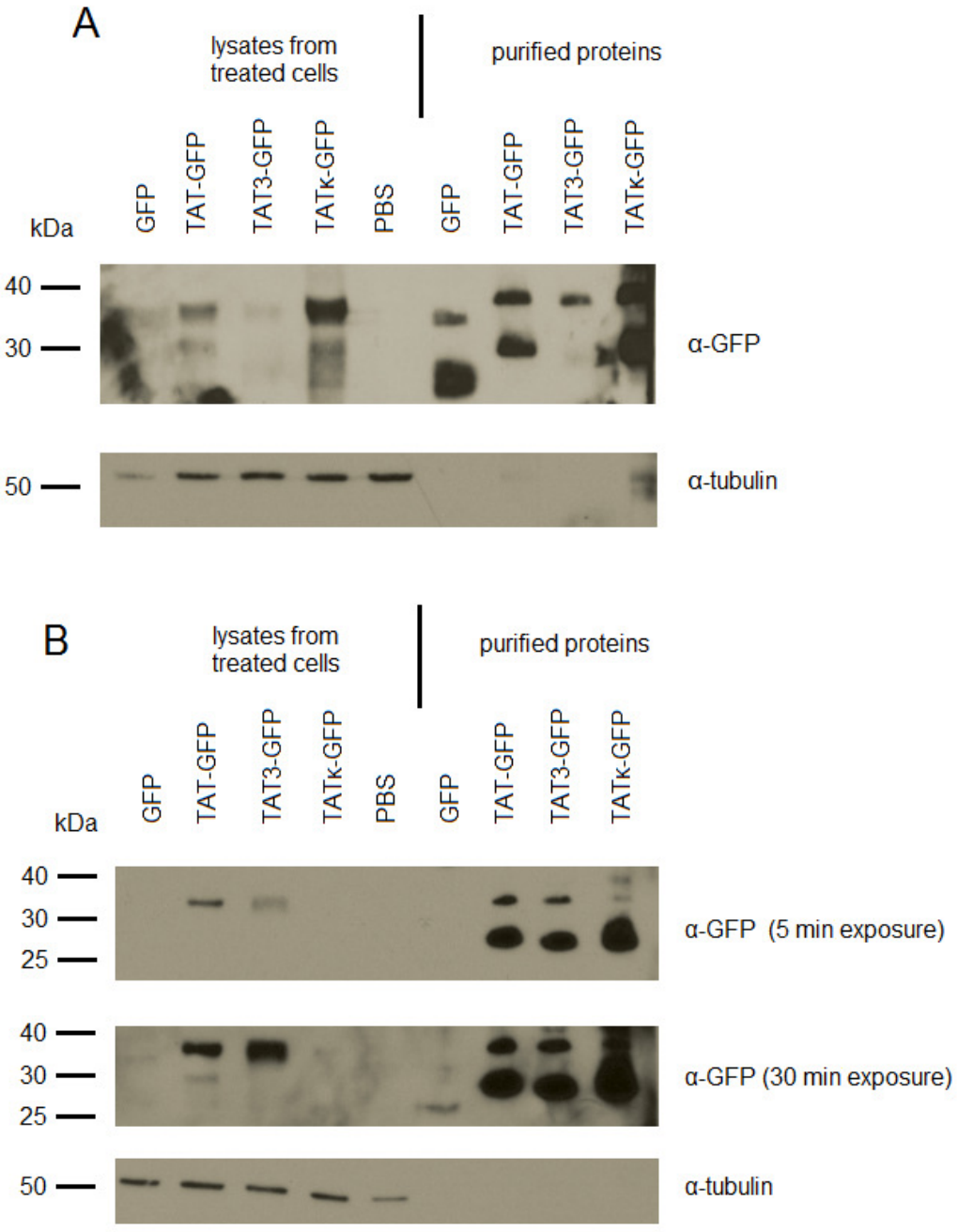
A
lysates from treated cells
purified proteins
GFP
TAT-GFP
TAT3-GFP
TATκ-GFP
PBS
GFP
TAT-GFP
TAT3-GFP
TATκ-GFP
kDa
40
30
α-GFP
50
α-tubulin
B
lysates from treated cells
purified proteins
GFP
TAT-GFP
TAT3-GFP
TATκ-GFP
PBS
GFP
TAT-GFP
TAT3-GFP
TATκ-GFP
kDa
40
30
25
α-GFP (5 min exposure)
40
30
25
α-GFP (30 min exposure)
50
α-tubulin

**Figure 3.9:** Transduction of bacterial TAT-GFP proteins *in vivo*. Treated cells were lysed and separated by electrophoresis with samples of the GFP and TAT-GFP aliquots used to treat the cells and subjected to immunoblotting using a rabbit α-GFP antibody. Western blots from two experiments (Panels A and B) show the consistency of TAT-GFP and TAT3-GFP and the inconsistent nature of TATκ-GFP, which is present in the lysate of treated cells in Panel A but absent in Panel B.

### 3.3: Adenoviral constructs and SP-SMN secretion

#### 3.3.1: Introduction

Transient transfection of constructs encoding SP-TAT-SMNs did not allow for clear assessment of secretion and subsequent uptake of these proteins (Figure 3.5). We developed an adenovirus-based system in which cells infected by the Ad vector produced and secreted large quantities of the fusion proteins. Conditioned media from the infected cells was used to assess secretion efficiency via protein precipitation or filtered and applied to uninfected cells to observe cellular uptake of the secretion proteins. Figure 3.10 presents schematic representations of the SMN-encoding fragments inserted into the adenoviral genome.

#### 3.3.2: Expression of AdSP-TAT-SMNs

Having generated data suggesting that at least two of the TAT PTDs (TAT3 and TATκ) could be used effectively with the secretory peptide, and that the secretory peptide was functional in GFP fusions, we transitioned into an adenoviral system to investigate the secretion of SP-SMN fusions. We first generated three E1-deleted adenoviruses: JB131, which encodes SP-SMN; JB132, encoding SP-TAT3-SMN; and JB133 which encodes SP-TATκ-SMN. The SMN in all three constructs features a FLAG tag so that exogenous SMN can be distinguished from the endogenous SMN found in cell cultures by immunoblot. A549 cells were plated in 35 mm dishes and grown to confluency, then infected with the viruses at an MOI of 100 (~1.2 x $10^8$ pfu) in PBS at a total volume of 100 μL for 1 hour at 37ºC. After 1 hour, 2 mL of 10% FBS media was added and the cells were incubated for 17 hours. Cells were washed with PBS and then lysed and collected in 2x Laemmli buffer. Lysates were separated using 12% SDS-PAGE and subjected to

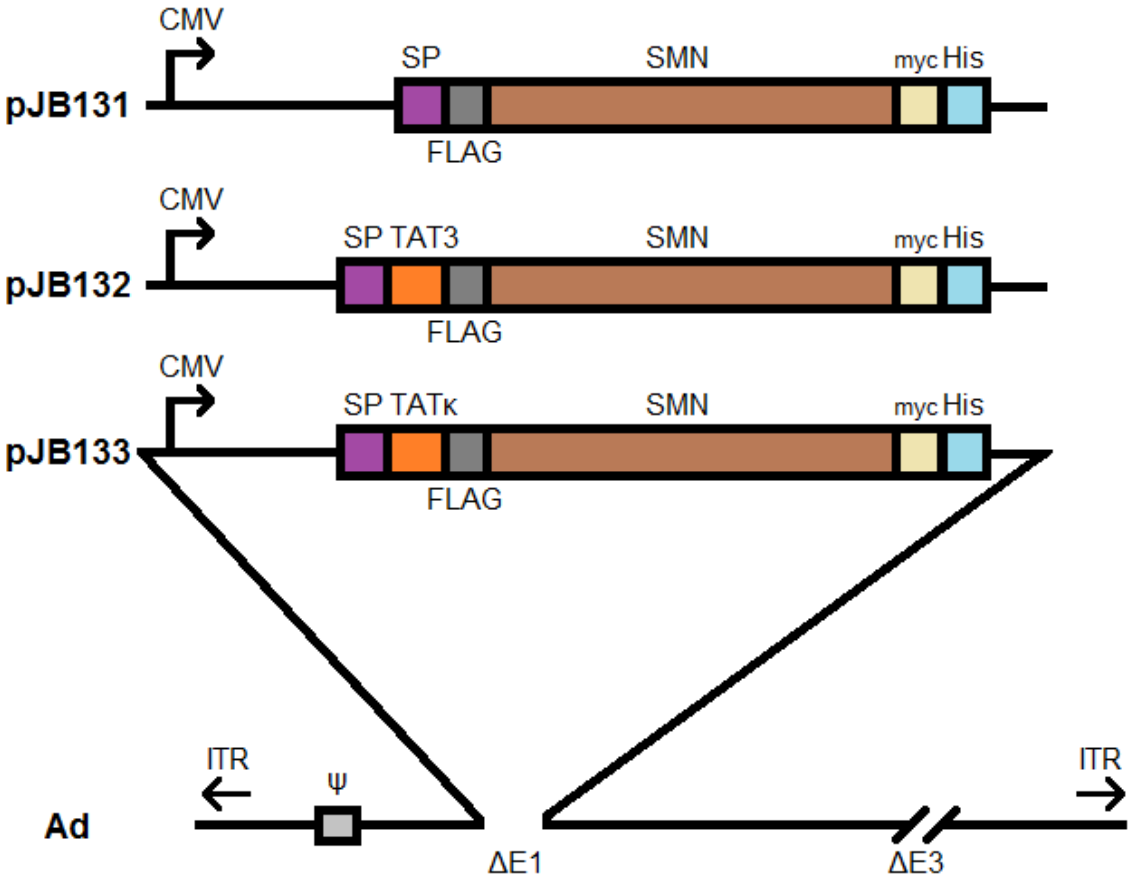
CMV
SP
SMN
myc His
pJB131
FLAG
CMV
SP TAT3
SMN
myc His
pJB132
FLAG
CMV
SP TATκ
SMN
myc His
pJB133
FLAG
ITR
ψ
ITR
Ad
ΔE1
ΔE3

**Figure 3.10:** Schematic representation of adenoviral constructs. These DNA fragments were inserted into the Ad genome by RecA-mediated recombination in place of the deleted E1 proteins. ITR refers to the inverted terminal repeats at either end of the adenoviral genome. ψ denotes the viral packaging element.

Western blotting. Expression of the viral SMN was assessed using an α-FLAG antibody (Figure 3.11). Addition of a TAT PTD caused an upward shift of about 5 kDa in our GFP fusions, so the expected size of TAT-SMNs was approximately 43 kDa. Appropriate bands are found in Figure 3.11 in the AdSP-TAT3-SMN and AdSP-TATκ-SMN lanes, however there are also bands at the expected size of an unmodified FLAG-tagged SMN (~38kDa). This may indicate the retention and activity of the start codon located immediately before the FLAG sequence. Translation initiating at this ATG would generate a FLAG-SMN without an SP or a PTD. SMN signals present at 50 kDa in the AdSMN lanes may be caused by a missplicing event which incorporates peptides downstream of SMN in the viral genome, described previously by our laboratory [148]. The fusion proteins appear to be expressed at comparable levels following infection with equal concentrations of virus.

### 3.3.3: Secretion and transduction of virally delivered SP-TAT-SMNs

In addition to cell lysates, media was collected from the dishes of infected cells and filtered using syringe filters. Filtered media was either subjected to TCA precipitation or passed through a 100 kDa size exclusion column to remove any residual virions prior to use in subsequent transduction experiments. Media precipitates were loaded alongside infected cell lysates for SDS-PAGE and Western blot analysis. The presence of SMN in the AdSP-SMN, AdSP-TAT3-SMN, and AdSP-TATκ-SMN media precipitates in Figure 3.12A suggests that the SP is functional in the viral vectors. However, the intensity of these signals is low compared to the signal yielded from the cell lysates, which may suggest that the SP is less efficient in these constructs than it was in the SP-GFPs.

To assess the transduction capability of the fusion SMNs after secretion, we applied media

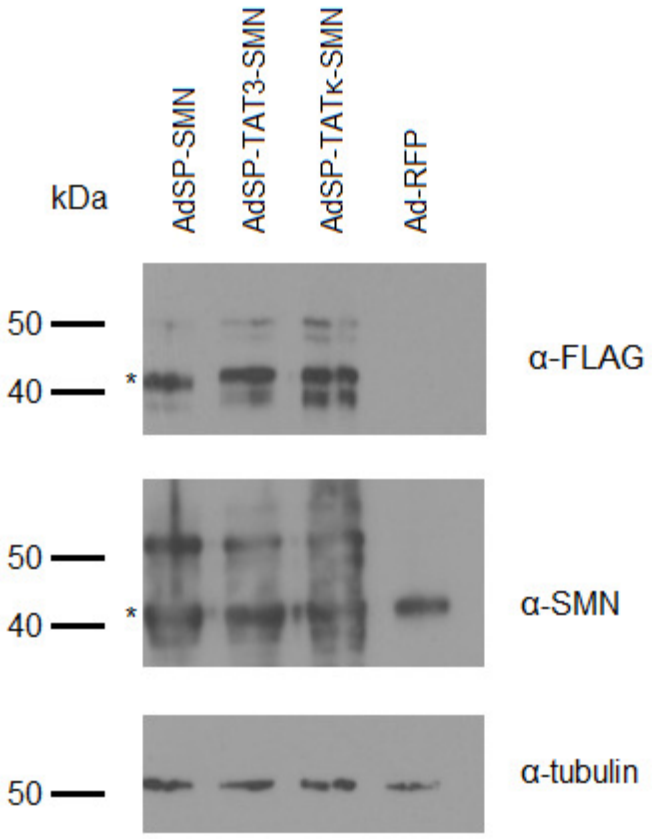
kDa
AdSP-SMN
AdSP-TAT3-SMN
AdSP-TATκ-SMN
Ad-RFP
50
40
*
α-FLAG
50
40
*
α-SMN
50
α-tubulin

**Figure 3.11:** Expression of adenoviral SP-SMN and SP-TAT-SMN proteins. Cells infected with AdSP-SMN, AdSP-TAT3-SMN, AdSP-TAT-SMN, or an AdRFP control virus at an MOI of 100 were incubated for 18 hours at 37ºC. After SDS-PAGE and Western blotting, of the infected cell lysates, the membrane was probed α-FLAG to detect expression of the viral SMN construct. An α-SMN antibody was used to verify the expected size difference between TAT-SMNs and endogeonous SMN. Asterisks indicate the expected size of the fusion protein.

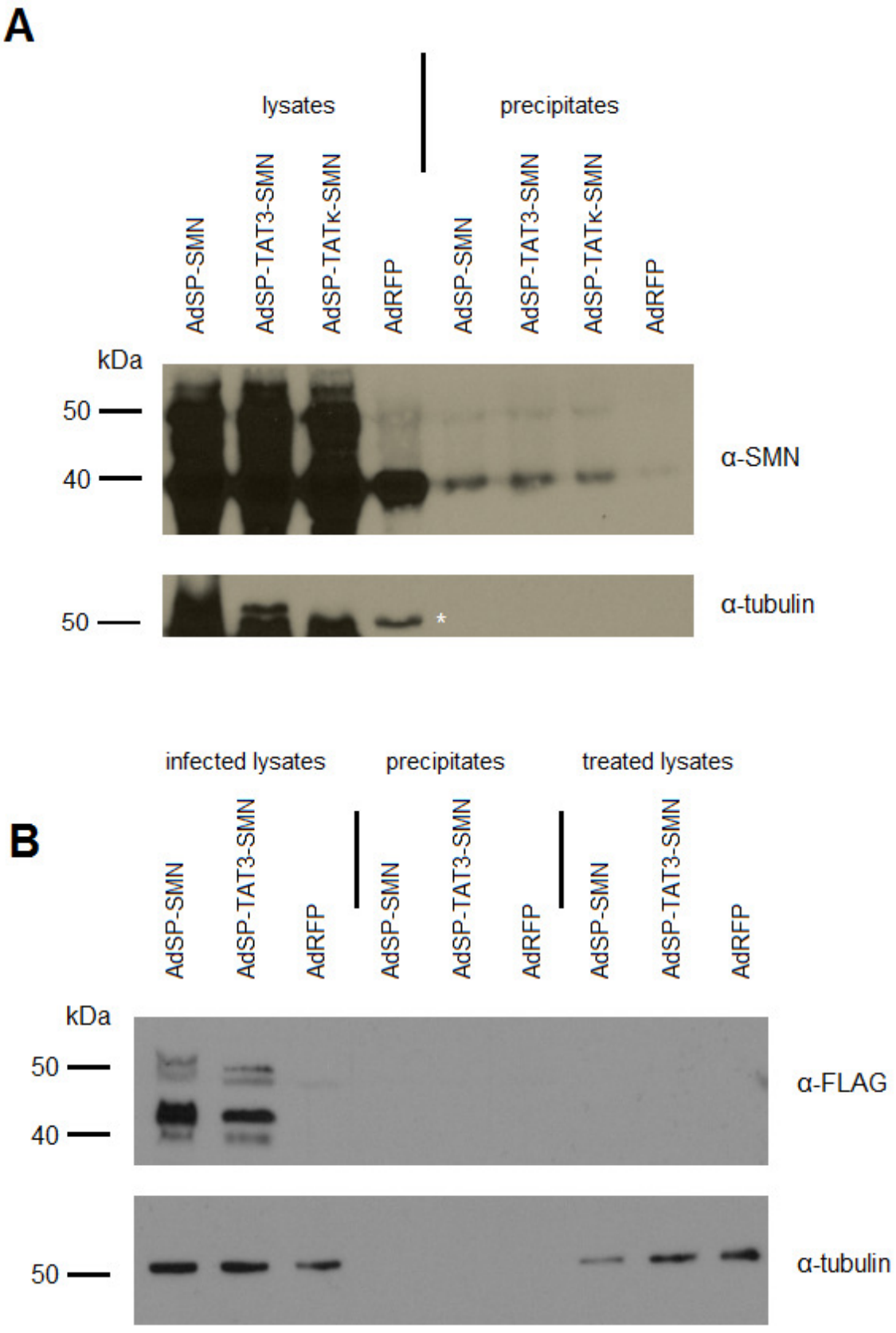
A
lysates
precipitates
AdSP-SMN
AdSP-TAT3-SMN
AdSP-TATκ-SMN
AdRFP
AdSP-SMN
AdSP-TAT3-SMN
AdSP-TATκ-SMN
AdRFP
kDa
50
40
α-SMN
50
*
α-tubulin
B
infected lysates
precipitates
treated lysates
AdSP-SMN
AdSP-TAT3-SMN
AdRFP
AdSP-SMN
AdSP-TAT3-SMN
AdRFP
AdSP-SMN
AdSP-TAT3-SMN
AdRFP
kDa
50
40
α-FLAG
50
α-tubulin

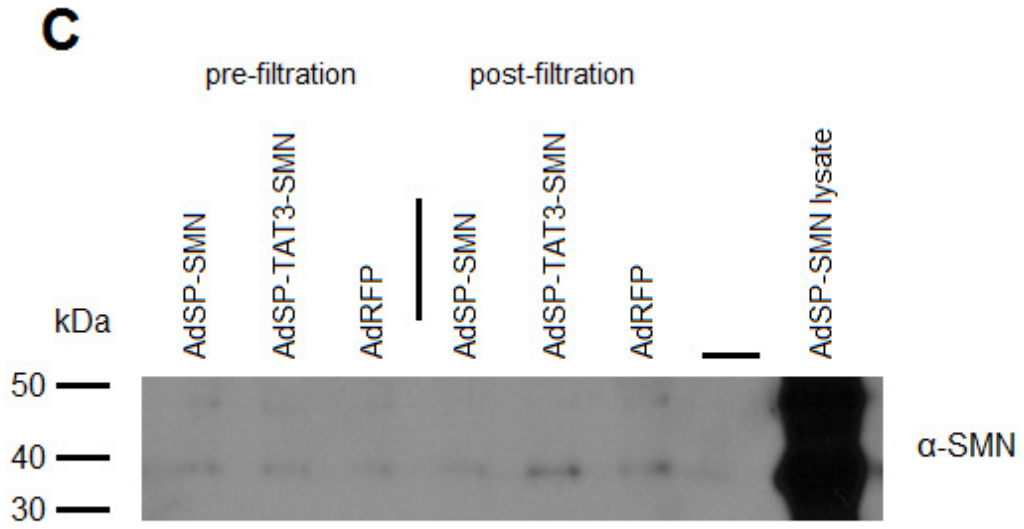
C
pre-filtration
post-filtration
AdSP-SMN
AdSP-TAT3-SMN
AdRFP
AdSP-SMN
AdSP-TAT3-SMN
AdRFP
AdSP-SMN lysate
kDa
50
40
30
α-SMN

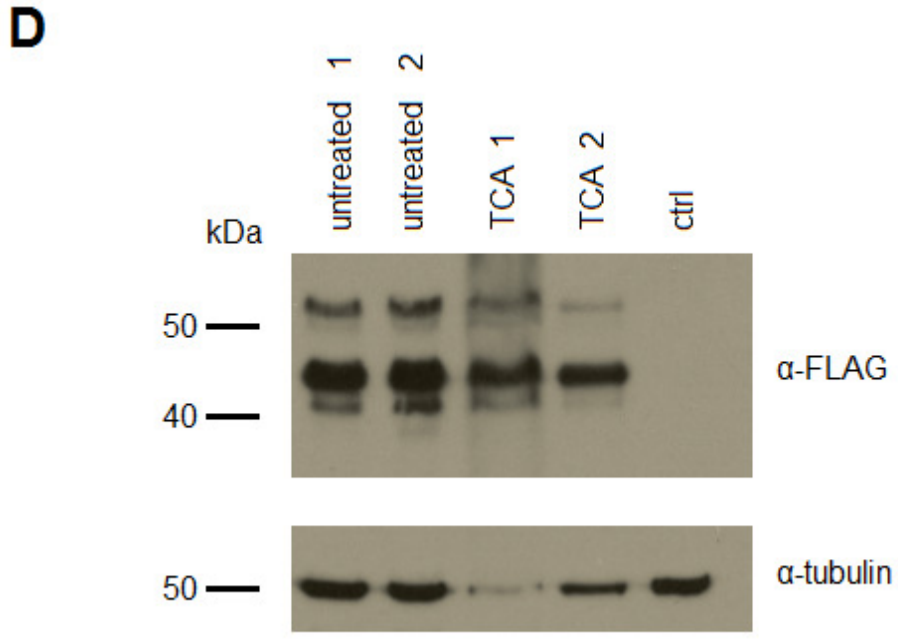
D
untreated 1
untreated 2
TCA 1
TCA 2
ctrl
kDa
50
40
α-FLAG
50
α-tubulin

**Figure 3.12:** Secretion and transduction of virally delivered SP-SMN and SP-TAT-SMN proteins. Panel A: Cell lysates and media were collected after infections with AdSP-SMN, AdSP-TAT3-SMN, AdSP-TATκ-SMN, and AdRFP at an MOI of 100 for 18 hours. Asterisk indicates the correct band for tubulin, as the secondary antibody recognized a previously applied antibody after stripping. Panel B: The Western blot indicates that SMN is present in the media precipitates. Infected cell lysates were electrophoresed with media precipitates and lysates from media-treated cells. Panel C: Media precipitates from unfiltered and filtered media were electrophoresed together and subjected to immunblotting. Comparable signals were obtained for all viruses under both conditions when probed α-SMN. Panel D: Cells were infected with AdSP-SMN and lysates were collected in Laemmli buffer (untreated) or treated with TCA prior to being collected in Laemmli buffer (TCA) along with uninfected cell lysates (ctrl). Comparable α-FLAG signals suggest that TCA does not affect detection of the tag.

which had been filtered and passed through a size exclusion column to a new population of A549 cells for 2 hours at 37ºC. Following washes with PBS, trypsin, 10% media, and PBS once more, the treated cells were lysed and collected in Laemmli buffer. SDS-PAGE and Western blot analysis of lysates from the initially infected cells, protein precipitates from the post-incubation media, and lysates of the media-treated cells (Figure 3.12B) suggests that none of the TAT-SMN fusion proteins successfully transduces the media-treated cells. While there appears to be no TAT-SMN in the media precipitates when probed with α-FLAG, this was consistent with an ongoing difficulty to detect secreted protein using this antibody. The presence of SMN in the media is verified by Figure 3.12C, which also addresses our concern that the filtration and/or size exclusion process was causing excessive loss of the secreted protein. The amount of SMN present in the media before and after the filtration process is approximately equivalent. Therefore, the TAT-SMN fusion proteins are absent in the media-treated cells, but this is not caused by protein loss during filtration of the media.

As described above, we experienced difficulty with detecting secreted FLAG-tagged proteins by Western blot using an α-FLAG antibody. In Figure 3.12D we addressed the concern that treatment with TCA might alter the FLAG tag such that it is not recognized by the antibody. A549s were infected with AdSP-SMN for 18 hours, after which the infected cells were collected in Laemmli buffer or treated with 200 μL of 100% w/v TCA for 2 minutes, then washed with PBS and collected in Laemmli buffer. The TCA-treated and untreated lysates were subjected to SDS-PAGE and Western blotting. Figure 3.12D indicates that there is no significant difference between the α-FLAG signals of the TCA-treated lysates versus those of the untreated lysates, though the first duplicate of the TCA-treated lysates yields a weaker α-tubulin signal than the other samples.

### 3.3.4: Recovery of SMN from media of uninfected cells

During many experiments in which we precipitated proteins from media, we were able to detect SMN in media from untreated cells, suggesting that it may be released naturally from the cell. An experiment designed to reproduce this observation is presented in Figure 3.13A. A549 cells were grown to confluency in a 6-well plate. Once the cells were confluent, the cells were washed with PBS and fresh 10% FBS media was applied. The cells were incubated in the new media for 24 hours at 37ºC. The media was collected from the cells and subjected to protein precipitation using TCA. All six samples in Figure 3.11A yielded a faint band of approximately 38 kDa when probed with an α-SMN antibody. None of these precipitates yielded a band when probed with α-tubulin, which suggests that the SMN signal is not due to cell death. To address the possibility that the α-SMN antibody was cross-reacting with protein in the FBS, we applied three dilutions of FBS (1x, 0.1x, 0.01x) in PBS to a 12% SDS-PAGE gel and performed an immunoblot using the same α-SMN antibody (Figure 3.13B). The absence of a clear band in any of the serum lanes suggests that the SMN signal yielded from untreated media precipitates is not caused by cross-reactivity with serum proteins. The bands which appear on the 1x and 0.1x serum lanes in Figure 3.13B are not likely to be real bands as they are not the expected width or shape for a band derived from a 10-well acrylamide gel. These bands were not present at all in a second replicate of this experiment. We also investigated whether this secretion occurs in cells derived from *Smn*$^{2B/-}$ mice and wild-type littermates. In the *Smn*$^{2B/-}$ model, affected mice have one allele of *Smn* knocked out and the other contains a mutation in an ESE in exon 7 of *Smn,* which causes this exon to be preferentially excluded from the transcript [77,149]. These mice exhibit an

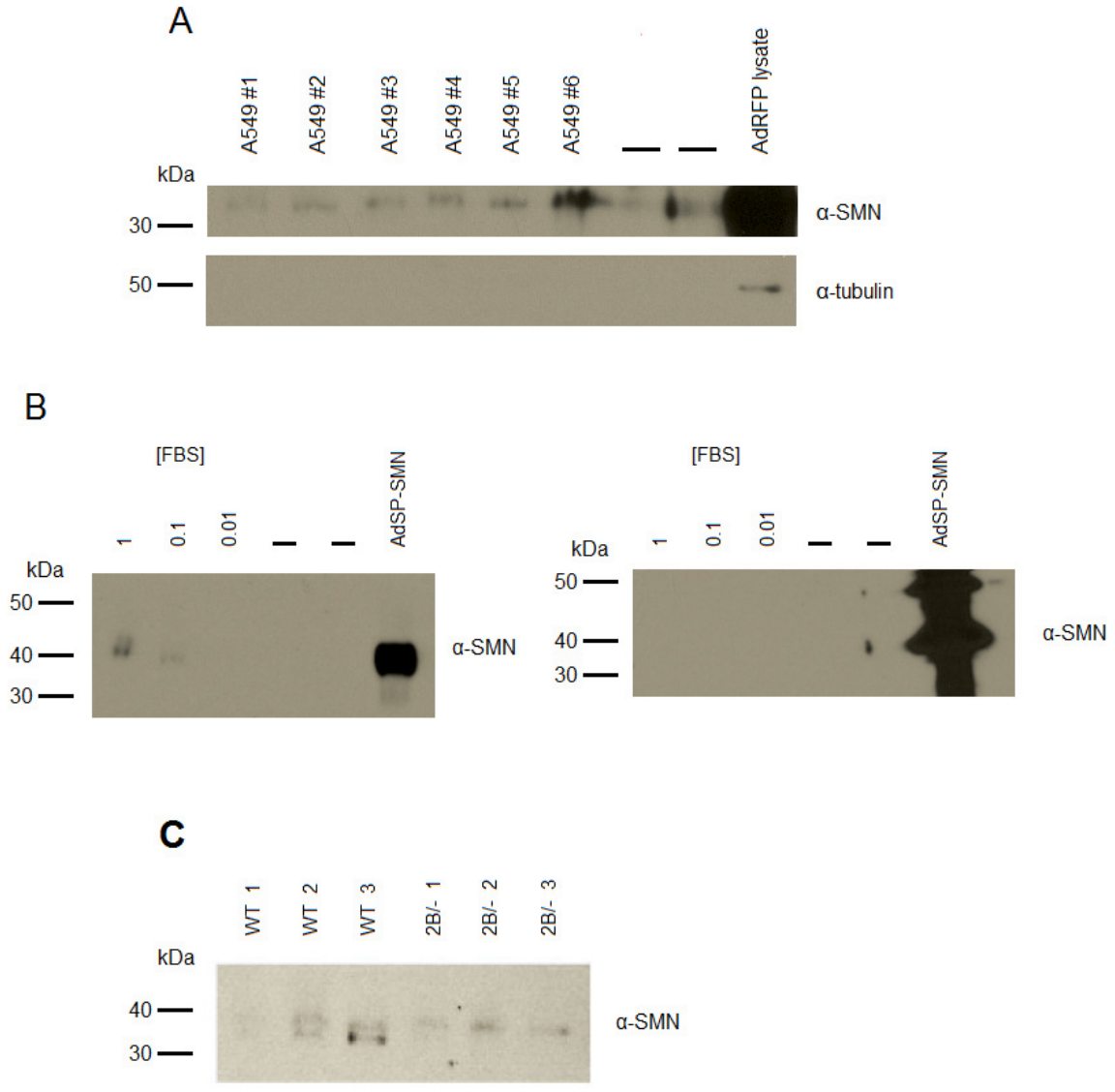
A
A549 #1
A549 #2
A549 #3
A549 #4
A549 #5
A549 #6
AdRFP lysate
kDa
30
50
α-SMN
α-tubulin
B
[FBS]
1
0.1
0.01
AdSP-SMN
kDa
50
40
30
α-SMN
[FBS]
1
0.1
0.01
AdSP-SMN
kDa
50
40
30
α-SMN
C
WT 1
WT 2
WT 3
2B/- 1
2B/- 2
2B/- 3
kDa
40
30
α-SMN

**Figure 3.13:** Recovery of SMN from media of untreated cells. Six wells of A549 cells were subjected to a media change and incubated for 24 hours at 37ºC. The media was collected from each and precipitated using TCA. Panel A: Following 12% SDS-PAGE, the Western blot was probed α-SMN. Faint bands in each lane corresponding to the numbered A549 replicates (A549 #1-6) suggest that SMN is present in the precipitate. The two lanes marked with an underscore were left blank to minimize signal bleeding from the AdRFP-infected positive control. For this latter treatment, we are only detecting endogenous protein inside the cell. Panel B: Three dilutions of FBS (1x, 0.1x, and 0.01x) were separated by SDS-PAGE and subjected to Western blotting. Panel C: Media used to culture mouse embyronic fibroblast (MEF) cells derived from wild-type (WT) or intermediate SMA mice (2B/-) was collected and subjected to TCA protein precipitation. The protein precipitates were separated by SDS-PAGE and analyzed by immunoblot.

intermediate SMA phenotype which manifests after post-natal day 10 and has a median lifespan of 28 days [77]. Therefore, if secretion of endogenous SMN occurs, we expected to see less SMN in the media of cells derived from *Smn*$^{2B/-}$ mice compared to their wild-type littermates. Media used to culture mouse embryonic fibroblasts (MEFs) derived from wild-type or *Smn*$^{2B/-}$ mice was precipitated using TCA and subjected to SDS-PAGE and Western blotting. Probing with α-SMN resulted in two bands in the lanes corresponding to the WT MEFs and only one in the SMA MEFs. It is possible that the band of lower molecular weight, which is absent in the SMA MEFs, represents endogenously secreted SMN, though the band common to all lanes more closely matches the expected 38 kDa size of the protein. Taken together, these data suggest that the secretory peptide may not be necessary for SMN to escape the cell, and endogenous SMN may be released from the cell under normal circumstances.

### 3.3.5: Conclusion

The data presented in Figure 3.12 suggests that the secreted proteins are not transducing the recipient cells, but protein loss during filtration is not the cause of this, nor is insufficient expression of the fusion proteins (Figure 3.11). Curiously, secretion of endogenous SMN may occur in the absence of the signal peptide or any kind of exogenous construct (Figure 3.13).

# Chapter 4 – Discussion and Future Directions

Spinal muscular atrophy is a frequently lethal disease that exhibits early onset in its most common and most severe form. Early intervention appears to be essential in alleviating the disease phenotype [42-44], which manifests not only in α-motor neurons but also in peripheral tissues. Restoration of SMN protein levels in the CNS or in peripheral tissues has been shown to rescue phenotype *in vivo* [100]. In the present work we sought to develop a secretable TAT-SMN fusion protein delivered by an adenovirus. In theory, the adenovirus would infect the liver when delivered intravenously. Hepatocytes would express and secrete the TAT-SMN protein which would be taken up from the blood by peripheral tissues and would cross the blood-brain barrier using the TAT PTD. This therapeutic would allow for widespread restoration of SMN protein levels while avoiding the dosing concerns of direct protein injections to the CNS. In the present work we used GFP fusions to compare the efficacy of TAT-PTD variants and to test the function of the secretory peptide in combination with these PTDs. We developed adenoviral vectors encoding SP-TAT-SMNs to investigate the functionality of these peptides with an SMN fusion and began to assess functional rescue using these vectors.

## 4.1: TAT-GFPs can be generated in mammalian and bacterial cells with varying yields.

We were able to generate all of the TAT-GFP and SP-TAT-GFP proteins we sought to generate in both mammalian cells and in *E. coli*; however, the amount of protein generated by transfection or transformation of 5 μg of plasmid varied considerably among plasmids within the same system. There is an apparent difference in Figure 3.2 between the yield of TAT-GFP versus TAT3-GFP, TATκ-GFP, and the control GFP plasmid in the mammalian system. Also, the SP

fusion proteins which contain a TAT PTD yielded considerably weaker signals than the SP-GFP. The tubulin signals in Figure 3.2 suggest that the differences are not due to variations in the number of cells present or the amount of sample loaded, but rather in the transfection efficiency of each plasmid or in the degree to which each construct was expressed following transfection. It is possible that different amounts of each construct were transfected if the quantification of the large-scale plasmid preparations was incorrect, however these concentrations were determined by spectroscopy and are believed to be accurate.

In the bacterial system we initially encountered inconsistency in the expression of JB107 following IPTG induction and the original GFP and TAT-GFP constructs were not expressed at all. We generated new constructs by replacing TATκ in the functional TATκ-GFP construct with the other TAT variants or removing it. The new plasmids were consistently expressed following induction, but the yield of the control GFP was much lower than the TAT-GFPs in all instances in which we prepared these proteins. This meant that we had to dilute the purified TAT-GFP proteins in order to perform experiments with a comparable amount of all proteins. The diluted TAT-GFPs still allowed us to observe and compare transduction of the fusion proteins, however it is possible that the proteins may have behaved differently at higher concentrations or that one TAT PTD would be more obviously superior to the others if the experiments were performed using higher concentrations.

### 4.2: All three TAT PTDs appear to be functional, but TAT3 appears to be best suited for our therapeutic protein.

After verifying the expression of the TAT-GFP fusion proteins in mammalian cells, we initially attempted to compare the transduction capability of the three TAT PTD variants in the

same system using a simple freeze-thaw lysis of transfected cells and treatment of new 293 cells using these lysates (Fig. 3.3). However, we found that this approach yielded inconsistent results between replicates and presented challenges in controlling the amount of protein applied during the treatment. In some cases the TAT-GFP concentration was so low in the transfected lysates that it was not visible on the Western blot. We began working with a bacterial system in order to produce large pools of protein that could be diluted to be approximately equivalent to one another in concentration. Though we successfully generated TAT-GFPs using IPTG-induced constructs (Fig. 3.7A), the bacteria also consistently expressed "unmodified" GFP (GFP without a TAT PTD or an SP), likely starting at the eGFP start codon which was still present in the plasmid. Purifying the protein preparations using nickel columns removed some, but not all contaminating proteins, and the unmodified GFP remained bound to the column until the elution stage because the 6x histidine tag is present at the C terminus regardless of which start codon is used (Fig. 3.7B).

After normalizing the concentrations of TAT-GFPs, we treated A549 cells with the proteins to determine whether or not they were capable of transduction and to compare their relative transduction efficiency. In the initial experiments we used 293 cells, but we found these cells too readily detached from the plate during treatment or during the trypsin wash. A549 cells do not detach as easily and were substituted for the majority of these experiments. Trypsin was included in the wash in order to remove any GFP that might have adhered to the surface of the treated cells but had not penetrated the cell membrane; however, this measure appears to be ineffective as we still observed bands corresponding to the unmodified GFP in some of the protein-treated cell lysates (Figure 3.9). Faint fluorescence can be seen in the microscopy image for GFP (Fig 3.8) as well, which we observed following most treatments, particularly in areas containing detaching cells and other debris. The length of incubation in trypsin may not have been long enough or trypsin may be ineffective for detaching these proteins from cell surfaces.

The microscopy images suggest that all three TAT-GFPs penetrate cell membranes to a greater degree than the control GFP. The punctate pattern of green fluorescence was a preliminary indication that the TAT-GFPs may also be localizing in the nucleus, which would be expected considering the inherent nuclear localization properties of TAT [138]; we attempted to stain the protein-treated cells with Hoechst stain to determine whether or not this occurred but this approach was not successful. Though TAT-GFP was generally produced in the largest quantity, after normalization it appeared to be less effective than TAT3-GFP and TATκ-GFP.

We supported the microscopy data using Western blots (Fig. 3.9) to allow for a more direct comparison between the TAT PTD variants and to perform a secondary check for transduced protein if none was visibly apparent by microscopy. The Western blots supported the observation that the three TAT-GFPs appeared to penetrate the cell membranes, however the trend in efficiency was reversed regarding TAT-GFP and TAT3-GFP, as TAT3-GFP appears to be slightly less efficient than the others on the Western blots. Curiously, TATκ-GFP did not yield any GFP signal at all in treated cell lysates in some of the Western blots after minimal fluorescence was observed by microscopy. This suggests that TATκ-GFP is unreliable regarding its ability to cross cell membranes, though it appears to be the most effective TAT variant of the three when transduction succeeds. At this point we decided we would continue working with all three TAT PTD variants, as all three appear to have at least some transduction capability though our TATκ PTD may be problematic at a later stage.

### 4.3: Viral SP-SMNs are expressed following infection with similar yields.

When we infected A549 cells at MOI 100, the fusion SMN encoded by each of the three adenoviral vectors appear to be expressed to a comparable degree (Fig. 3.7). Curiously, the

endogenous SMN in the AdRFP lane of Figure 3.7 appears to be similar in size to the fusion SMNs in the first three lanes. This appears to be isolated to this figure, as the SMN in AdRFP-infected lysates appears to be the same size as endogenous SMN (~38 kDa) in Figure 3.12A and Figure 3.13A.

### 4.4: Secretory peptide appears to be functional in SP-TAT-GFPs but may not function in viral vectors.

Following transfection with the SP-GFP and SP-TAT-GFP plasmids, we were able to precipitate GFPs and TAT-GFPs from the media of cells transfected with all constructs except for SP-TAT-GFP (Fig. 3.4). The absence of tubulin in the media precipitates indicates that the presence of GFP in media is unlikely the result of cell lysis. Though we were concerned that the TAT PTD of this fusion protein would be cleaved by furin during secretion, cleavage of the PTD should not affect recognition of the protein by the α-GFP antibody. Therefore, we suspect that the combination of the native TAT PTD and the secretory peptide may cause improper localization as the nuclear localization tendency of the PTD conflicts with the Golgi secretion signal of the SP. Though TATκ-GFP could be consistently recovered from media, the yield of this protein was less than that of TAT3-GFP. Combining our observations regarding TAT PTD transduction capability and recovery of secreted proteins from media suggests that TAT3 is likely the most effective PTD for our purposes.

Due to the inability to recover SP-TAT-GFP from media, we chose to forgo the use of the native TAT PTD in our adenoviral constructs. We generated viruses encoding SP-SMN, SP-TAT3-SMN, or TATκ-SMN tagged with FLAG and verified the expression of the fusion proteins in infected cells (Fig. 3.11) prior to assessing the presence of secreted SMN in the media of infected

cells. Our initial experiments suggested that the SP was functioning in these constructs, though at a diminished capacity compared to that observed in the SP-GFP proteins. SMN was recovered from the media of infected cells, but in concentrations that yielded faint signals which deviated from the expected size of the fusion protein as observed in infected lysates (Fig 3.12A).

While investigating media precipitates for the presence of our fusion SMN proteins we found that the proteins could not be detected when we performed immunoblots using an α-FLAG antibody. Initially we were concerned that the protein precipitation protocol may alter the FLAG tag such that the antibody cannot recognize it. Specifically, we sought to investigate the effect of TCA treatment on α-FLAG signal by harvesting cells which had been infected with AdSP-SMN with or without a brief TCA treatment (Fig. 3.12D). The α-FLAG signals were equally strong in all four samples, suggesting that TCA treatment does not render the FLAG tag unrecognizable by the antibody. The loss of α-FLAG signal we observed following secretion may be consistent with recent work by Schmidt *et al* which indicated that the functionality of the FLAG tag was lost following secretion in insect cells [150].

Data generated during the SP-GFP phase of this work suggested that the secretory peptide was functional in most of the SP-GFP and SP-TAT-GFP fusion proteins. Preliminary assessments of the virally delivered fusion proteins suggested that the SP was functional in those proteins as well, however the inability to detect the FLAG tag in protein precipitates and data from later experiments began to cast doubt on the efficacy of the secretory peptide in our viral vectors.

### 4.5: Transduction of SP-TAT-SMNs does not occur following secretion.

Although our data suggest that the viral proteins are expressed (Fig. 3.11) and are secreted into media following infection (Fig. 3.12A), we were unable to detect our fusion protein in cells

treated with media from cells infected with the adenoviral vectors. In Figure 3.12B we observe no FLAG signal in the treated cell lysates, despite the indication that SMN is present in the media precipitates (Fig. 3.12C) before and after application to the 100 kDa size exclusion column. The media precipitates in Figure 3.12B are the same samples analyzed in Figure 3.12C, and the absence of tubulin signals in these lanes in panel B suggests that the SMN signals in panel C are not the result of cell death and lysis releasing SMN into media. Though the difference was not quantified, there appears to be minimal loss of SMN protein during the size exclusion purification. Curiously, the strength of the SMN signals in the AdSP-SMN and AdSP-TAT3-SMN lanes are similar to that of the AdRFP lane. This suggests that the SP was not enhancing the secretion of the fusion proteins in this instance. The presence of SMN signal in the AdRFP media precipitates may be the result of the apparent secretion of unmodified endogenous SMN suggested by Figure 3.13. If this is the case, then it is likely that the majority of the SMN found in any of the lanes in Figure 3.12C is endogenous SMN, and that the secretory peptide was not functioning.

Attempting to visualize the secretion and transduction of GFP-tagged TAT-SMNs yielded similar results (Fig. 3.5). We sought to identify cells that contained GFP but not RFP: the SP-TAT-SMNs were fused to a GFP, and RFP was present on the same plasmid that encoded the fusion proteins. Therefore, the presence of RFP in a cell indicates that it had been transfected and any GFP-tagged fusion SMNs present were most likely synthesized within that cell. The presence of GFP in the absence of RFP would indicate that the cell was not transfected and could not generate the fusion proteins, but had received the fusion proteins via secretion from a transfected cell and subsequent transduction of the proteins across its cell membrane. Examples like the one shown in Figure 3.5 were rare, and in all cases the green cell was adjacent to a cell which was both red and green. Therefore, we cannot dismiss the possibility that the transfected cell simply divided after

expressing the fusion protein. The fact that experiments involving the transfer of conditioned media rather than transfected cells yielded no green cells supports this explanation. This methodology did not allow us to determine whether the issue lies with the TAT PTD or the SP; however, these observations combined with those from Figure 3.12 suggest that the secretory peptide may not be functional in the SMN fusions.

Our data suggest that the vectors as designed do not succeed in delivering their therapeutic proteins *in vitro*. Though our data seem to indicate that the secretory peptide is not functional in these proteins (or does not function consistently), based on the experiments performed to date we cannot conclude whether or not the TAT PTDs are functional in these proteins either. Recent work by Shen *et* al indicated that the transduction capability of an SP-TAT-Cherry fusion was significantly diminished following ER/Golgi secretion [151]. The same fusion protein could efficiently transduce cells if it was released via cell lysis rather than secretion, suggesting that the TAT PTD may be modified in some way during secretion such that its transduction capability is severely inhibited. This observation was not limited to Cherry protein fusions, as the group repeated the experiment replacing Cherry with a double V5 tag and this SP-TAT-V5V5 protein displayed the same reduction in transduction efficiency following secretion [151]. Therefore, we must consider the possibility that our TAT-SMN fusions will have diminished transduction capability following secretion and may not have been secreted in large enough amounts in our experiments to observe any transduction into the treated cell population. The transduction capability alone of the therapeutic proteins will need to be assessed in future work concurrent with further testing or redesign of the secretory peptide.

**4.6: SMN may be secreted in the absence of a secretory peptide.**

While we were analyzing the media of transfected and infected cells for the presence of secreted fusion proteins, we observed SMN in the media of untreated control cells such as those in Figure 3.13A. The absence of tubulin in these precipitates suggests that the SMN did not enter the media via cell lysis. We were initially concerned that these signals might be the result of cross-reactivity of the α-SMN antibody with a protein in FBS; however, the Western blot of a range of concentrations of FBS probed α-SMN shown in Figure 3.13B suggests that this is not the case. These signals appear to be representative of real SMN in the media.

Our analysis of SMN using SignalP 4.1 (Technical University of Denmark, Brede, Denmark) suggested that the protein was poorly suited for ER-Golgi secretion, though recent work by Ting *et al* indicated that SMN is found associated with Golgi secretion vesicles [70]. While interaction with the α-coatamer (Cop-α) was previously known [152], a direct connection between SMN and the Golgi apparatus had not been established. Ting *et al* determined that global disruption of Golgi-mediated secretion resulted in axonal defects similar to those observed in SMN knockdown neurons. Further, they observed that the interaction between SMN and Cop-α appears to regulate secretion of SMN granules from the Golgi [70]. Considering this previously unknown association between the Golgi and SMN granules and an apparent mechanism for regulating SMN granule secretion, it is possible that such secretion also occurs as a pathway for extracellular transport of SMN. Further investigation is necessary to determine if this is the case. If true, this could allow for new therapeutic strategies such as overexpression of secretion-optimized SMN in peripheral tissues rather than direct treatment of the CNS, or in restoring or enhancing the secretion capability of endogenous SMN. Secretion of endogenous SMN may also present a new facet to understanding the pathology of the disease.

Interestingly, while we consistently observed SMN in the media of A549 and MN1 cells,

preliminary experiments in 293s suggested that the tentative secretion of endogenous SMN does not occur in those cells. It is presently unclear whether the apparent secretion is cell-specific and coincidentally occurs in both A549s and MN1s, or the lack of secretion is specific to 293s.

### 4.7: Future directions

Nuclear localization of the TAT-GFP fusion proteins can be verified using fluorescence microscopy and nuclear staining or with confocal microscopy. The results of such microscopy might reveal previously unseen differences in the nuclear localization capability of the three TAT variants.

The capability of the SP-TAT-SMN fusion proteins to be secreted by a producer cell population and taken up by a separate recipient population may be more efficiently investigated by culturing the two cell populations in the same well separated by a semi-permeable membrane. The membrane would allow for transmission of the secreted proteins to the recipient population while keeping the cell populations separated. This approach might allow for longer expression of the introduced construct and sustained treatment with the secreted protein. Transfer of SP-TAT-GFPs in this manner could be visualized by fluorescence microscopy and verified by immunblot, though the SMN fusion proteins could only be detected by immunoblot in this assay.

To verify restoration of SMN function and to provide another method to verify protein transfer we are continuing to seek an assay which clearly indicates the presence of functional SMN. This would provide us with a clear metric for the effectiveness of our therapeutic SMN proteins *in vitro*. Using this assay we could identify the best candidate vectors for the transition into *in vivo* experiments.

The observation that the secreted TAT-SMNs are not taken up by recipient cells following infection of producer cells with our Ad vectors may be explained by post-translational

modifications made to TAT during secretion that diminish its cell-penetrating capability [151]. Investigation into such modifications will reveal if this is the case and if further modifications can be made to the TAT PTD to prevent the loss of functionality.

Finally, to address the apparent secretion of endogenous SMN, we can treat untransfected, uninfected cells with brefeldin A to inhibit ER/Golgi protein secretion [153] and observe whether the apparent secretion persists.

### 4.8: Conclusion

In the present work we have compared the transduction capability of three TAT PTD variants and assessed the efficacy of a secretory peptide when fused to GFP. We selected the two most viable TAT PTDs and generated Ad vectors encoding secreted TAT-SMN fusion proteins. Our data suggest that TAT3 is the most suitable of the TAT variants for our therapeutic protein. The secretory peptide appeared to be functional in GFP fusions but may not be functional in the Ad vectors. The fusion protein expressed following infection with the Ad vectors is not taken up by recipient cells. Further investigation is warranted to determine whether this is due to post-translational modification of the TAT PTD during secretion that renders it ineffective.

## References

(1) Crawford TO, Pardo CA. The neurobiology of childhood spinal muscular atrophy. Neurobiol Dis 1996;3(2):97-110.
(2) Prior TW. Carrier screening for spinal muscular atrophy. Genetics in Medicine 2008;10(11):840-842.
(3)Nurputra DK, Lai PS, Harahap NIF, Morikawa S, Yamamoto T, Nishimura N, et al. Spinal muscular atrophy: From gene discovery to clinical trials. Ann Hum Genet 2013.
(4) Shababi M, Lorson CL, Rudnik-Schöneborn SS. Spinal muscular atrophy: A motor neuron disorder or a multi-organ disease*?* J Anat 2013 (article in press).
(5) Boyer JG, Bowerman M, Kothary R. The many faces of SMN: Deciphering the function critical to spinal muscular atrophy pathogenesis. Future Neurology 2010;5(6):873-890.
(6) Rudnik-Schöneborn S, Stolz P, Varon R, Grohmann K, Schächtele M, Ketelsen U-, et al. Long-term observations of patients with infantile spinal muscular atrophy with respiratory distress type 1 (SMARD1). Neuropediatrics 2004;35(3):174-182.
(7) Russman BS, Melchreit R, Drennan JC. Spinal muscular atrophy: The natural course of disease. Muscle and Nerve 1983;6(3):179-181.
(8) Fischbeck KH, Souders D, La Spada A. A candidate gene for X-linked spinal muscular atrophy. Adv Neurol 1991;56:209-213.
(9) Harding AE, Thomas PK. Hereditary distal spinal muscular atrophy. A report on 34 cases and a review of the literature. J Neurol Sci 1980;45(2-3):337-348.
(10) Russman BS. Spinal muscular atrophy: Clinical classification and disease heterogeneity. J Child Neurol 2007;22(8):946-951.
(11) Lefebvre S, Bürglen L, Reboullet S, Clermont O, Burlet P, Viollet L, et al. Identification and characterization of a spinal muscular atrophy-determining gene. Cell 1995;80(1):155-165.
(12) Hahnen E, Forkert R, Marke C, Rudnik-Schöneborn S, Schonling J, Zerres K, et al. Molecular analysis of candidate genes on chromosome 5q13 in autosomal recessive spinal muscular atrophy: Evidence of homozygous deletions of the SMN gene in unaffected individuals. Hum Mol Genet 1995;4(10):1927-1933.
(13) Rochette CF, Surh LC, Ray PN, McAndrew PE, Prior TW, Burghes AHM, et al. Molecular diagnosis of non-deletion SMA patients using quantitative PCR of SMN exon 7. Neurogenetics 1997;1(2):141-147.
(14) Lorson CL, Hahnen E, Androphy EJ, Wirth B. A single nucleotide in the SMN gene regulates splicing and is responsible for spinal muscular atrophy. Proc Natl Acad Sci U S A 1999;96(11):6307-6311.
(15) Jodelka FM, Ebert AD, Duelli DM, Hastings ML. A feedback loop regulates splicing of the spinal muscular atrophy-modifying gene, SMN2. Hum Mol Genet 2010;19(24):4906-4917.
(16) Lorson CL, Strasswimmer J, Yao J-M, Baleja JD, Hahnen E, Wirth B, et al. SMN oligomerization defect correlates with spinal muscular atrophy severity. Nat Genet 1998;19(1):63-66.
(17) Burnett BG, Muñoz E, Tandon A, Kwon DY, Sumner CJ, Fischbeck KH. Regulation of SMN protein stability. Mol Cell Biol 2009;29(5):1107-1115.
(18) Cho S, Dreyfuss G. A degron created by SMN2 exon 7 skipping is a principal contributor to spinal muscular atrophy severity. Genes and Development 2010;24(5):438-442.
(19) Schrank B, Götz R, Gunnersen JM, Ure JM, Toyka KV, Smith AG, et al. Inactivation of the survival motor neuron gene, a candidate gene for human spinal muscular atrophy, leads to

massive cell death in early mouse embryos. Proc Natl Acad Sci U S A 1997;94(18):9920-9925.
(20) Hsieh-Li H, Chang J-G, Jong Y-J, Wu M-H, Wang NM, Tsai CH, et al. A mouse model for spinal muscular atrophy. Nat Genet 2000;24(1):66-70.
(21) Lim SR, Hertel KJ. Modulation of Survival Motor Neuron Pre-mRNA Splicing by Inhibition of Alternative 3' Splice Site Pairing. J Biol Chem 2001;276(48):45476-45483.
(22) Hofmann Y, Lorson CL, Stamm S, Androphy EJ, Wirth B. Htra2-Î²1 stimulates an exonic splicing enhancer and can restore full-length SMN expression to survival motor neuron 2 (SMN2). Proc Natl Acad Sci U S A 2000;97(17):9618-9623.
(23) Hofmann Y, Wirth B. hnRNP-G promotes exon 7 inclusion of survival motor neuron (SMN) via direct interaction with Htra2-β1. Hum Mol Genet 2002;11(17):2037-2049.
(24) Cartegni L, Krainer AR. Disruption of an SF2/ASF-dependent exonic splicing enhancer in SMN2 causes spinal muscular atrophy in the absence of SMN. Nat Genet 2002;30(4):377-384.
(25) Kashima T, Manley JL. A negative element in SMN2 exon 7 inhibits splicing in spinal muscular atrophy. Nat Genet 2003;34(4):460-463.
(26) Pedrotti S, Bielli P, Paronetto MP, Ciccosanti F, Fimia GM, Stamm S, et al. The splicing regulator Sam68 binds to a novel exonic splicing silencer and functions in SMN2 alternative splicing in spinal muscular atrophy. EMBO J 2010;29(7):1235-1247.
(27) Miyajima H, Miyaso H, Okumura M, Kurisu J, Imaizumi K. Identification of a cis-acting element for the regulation of SMN exon 7 splicing. J Biol Chem 2002;277(26):23271-23277.
(28) Singh NN, Singh RN, Androphy EJ. Modulating role of RNA structure in alternative splicing of a critical exon in the spinal muscular atrophy genes. Nucleic Acids Res 2007;35(2):371-389.
(29) Miyaso H, Okumura M, Kondo S, Higashide S, Miyajima H, Imaizumi K. An intronic splicing enhancer element in survival motor neuron (SMN) pre-mRNA. J Biol Chem 2003;278(18):15825-15831.
(30) Kashima T, Rao N, Manley JL. An intronic element contributes to splicing repression in spinal muscular atrophy. Proc Natl Acad Sci U S A 2007;104(9):3426-3431.
(31) Matthijs G, Devriendt K, Fryns J-P. The prenatal diagnosis of spinal muscular atrophy. Prenat Diagn 1998;18(6):607-610.
(32) Ogino S, Leonard DGB, Rennert H, Ewens WJ, Wilson RB. Genetic risk assessment in carrier testing for spinal muscular atrophy. Am J Med Genet 2002;110(4):301-307.
(33) Moulard B, Salachas F, Chassande B, Briolotti V, Meininger V, Malafosse A, et al. Association between centromeric deletions of the SMN gene and sporadic adult-onset lower motor neuron disease. Ann Neurol 1998;43(5):640-644.
(34) Van der Steege G, Grootscholten PM, Van der Vlies P, Draaijers TG, Osinga J, Cobben JM, et al. PCR-based DNA test to confirm clinical diagnosis of autosomal recessive spinal muscular atrophy 7. Lancet 1995;345(8955):985-986.
(35) Chen WJ, Dong WJ, Lin XZ, Lin MT, Murong SX, Wu ZY, et al. Rapid diagnosis of spinal muscular atrophy using high-resolution melting analysis. BMC Medical Genetics 2009;10.
(36) Little SE, Janakiraman V, Kaimal A, Musci T, Ecker J, Caughey AB. The cost-effectiveness of prenatal screening for spinal muscular atrophy. Am J Obstet Gynecol 2010;202(3):253.e1-253.e7.
(37) Prior TW, Snyder PJ, Rink BD, Pearl DK, Pyatt RE, Mihal DC, et al. Newborn and carrier screening for spinal muscular atrophy. Obstetrical and Gynecological Survey 2010;65(11):697-699.
(38) Orzalesi M, Danhaive O. Ethical problems with neonatal screening. Ann Ist Super Sanita 2009;45(3):325-330.
(39) ACOG committee opinion no. 432: Spinal muscular atrophy. Obstet Gynecol 2009;113(5):1194-1196.

(40) Andermann A, Blancquaert I, Beauchamp S, Déry V. Revisiting Wilson and Jungner in the genomic age: A review of screening criteria over the past 40 years. Bull World Health Organ 2008;86(4):317-319.
(41) Swoboda KJ, Prior TW, Scott CB, McNaught TP, Wride MC, Reyna SP, et al. Natural history of denervation in SMA: Relation to age, SMN2 copy number, and function. Ann Neurol 2005;57(5):704-712.
(42) Porensky PN, Mitrpant C, McGovern VL, Bevan AK, Foust KD, Kaspar BK, et al. A single administration of morpholino antisense oligomer rescues spinal muscular atrophy in mouse. Hum Mol Genet 2012;21(7):1625-1638.
(43) Foust KD, Wang X, McGovern VL, Braun L, Bevan AK, Haidet AM, et al. Rescue of the spinal muscular atrophy phenotype in a mouse model by early postnatal delivery of SMN. Nat Biotechnol 2010;28(3):271-274.
(44) Glascock JJ, Osman EY, Wetz MJ, Krogman MM, Shababi M, Lorson CL. Decreasing disease severity in symptomatic, Smn -/-;SMN2 +/+, spinal muscular atrophy mice following scAAV9-SMN delivery. Hum Gene Ther 2012;23(3):330-335.
(45) Lefebvre S, Burlet P, Liu Q, Bertrandy S, Clermont O, Munnich A, et al. Correlation between severity and SMN protein level in spinal muscular atrophy. Nat Genet 1997;16(3):265-269.
(46) Coovert DD, Le TT, McAndrew PE, Strasswimmer J, Crawford TO, Mendell JR, et al. The survival motor neuron protein in spinal muscular atrophy. Hum Mol Genet 1997;6(8):1205-1214.
(47) Dubowitz V. Chaos in classification of the spinal muscular atrophies of childhood. Neuromuscular Disorders 1991;1(2):77-80.
(48) Thomas NH, Dubowitz V. The natural history of type I (severe) spinal muscular atrophy. Neuromuscular Disorders 1994;4(5-6):497-502.
(49) Russman BS, Iannacone ST, Buncher CR, Samaha FJ, White M, Perkins B, et al. Spinal muscular atrophy: New thoughts on the pathogenesis and classification schema. J Child Neurol 1992;7(4):347-353.
(50) Feldkötter M, Schwarzer V, Wirth R, Wienker TF, Wirth B. Quantitative analyses of SMN1 and SMN2 based on real-time lightcycler PCR: Fast and highly reliable carrier testing and prediction of severity of spinal muscular atrophy. Am J Hum Genet 2002;70(2):358-368.
(51) Liu Q, Dreyfuss G. A novel nuclear structure containing the survival of motor neurons protein. EMBO J 1996;15(14):3555-3565.
(52) Fischer U, Liu Q, Dreyfuss G. The SMN-SIP1 complex has an essential role in spliceosomal snRNP biogenesis. Cell 1997;90(6):1023-1029.
(53) Kolb SJ, Battle DJ, Dreyfuss G. Molecular functions of the SMN complex. J Child Neurol 2007;22(8):990-994.
(54) Grimmler M, Otter S, Peter C, Müller F, Chari A, Fischer U. Unrip, a factor implicated in cap-independent translation, associates with the cytosolic SMN complex and influences its intracellular localization. Hum Mol Genet 2005;14(20):3099-3111.
(55) Wan L, Battle DJ, Yong J, Gubitz AK, Kolb SJ, Wang J, et al. The survival of motor neurons protein determines the capacity for snRNP assembly: Biochemical deficiency in spinal muscular atrophy. Mol Cell Biol 2005;25(13):5543-5551.
(56) Lerner MR, Boyle JA, Mount SM, Wolin SL, Steitz JA. Are snRNPs involved in splicing? Nature 1980;283(5743):220-224.
(57) Bühler D, Raker V, Lührmann R, Fischer U. Essential role for the tudor domain of SMN in spliceosomal U snRNP assembly: Implications for spinal muscular atrophy. Hum Mol Genet 1999;8(13):2351-2357.
(58) Battle DJ, Kasim M, Yong J, Lotti F, Lau C-, Mouaikel J, et al. The SMN complex: An assembly machine for RNPs. Cold Spring Harb Symp Quant Biol 2006;71:313-320.

(59) Liu Q, Fischer U, Wang F, Dreyfuss G. The spinal muscular atrophy disease gene product, SMN, and its associated protein SIP1 are in a complex with spliceosomal snRNP proteins. Cell 1997;90(6):1013-1021.
(60) Gabanella F, Butchbach MER, Saieva L, Carissimi C, Burghes AHM, Pellizzoni L. Ribonucleoprotein assembly defects correlate with spinal muscular atrophy severity and preferentially affect a subset of spliceosomal snRNPs. PLoS ONE 2007;2(9).
(61) Carrel TL, McWhorter ML, Workman E, Zhang H, Wolstencroft EC, Lorson C, et al. Survival motor neuron function in motor axons is independent of functions required for small nuclear ribonucleoprotein biogenesis. Journal of Neuroscience 2006;26(43):11014-11022.
(62) Pellizzoni L, Kataoka N, Charroux B, Dreyfuss G. A novel function for SMN, the spinal muscular atrophy disease gene product, in pre-mRNA splicing. Cell 1998;95(5):615-624.
(63) Zhang Z, Lotti F, Dittmar K, Younis I, Wan L, Kasim M, et al. SMN Deficiency Causes Tissue-Specific Perturbations in the Repertoire of snRNAs and Widespread Defects in Splicing. Cell 2008;133(4):585-600.
(64) Bäumer D, Lee S, Nicholson G, Davies JL, Parkinson NJ, Murray LM, et al. Alternative splicing events are a late feature of pathology in a mouse model of spinal muscular atrophy. PLoS Genetics 2009;5(12).
(65) Fan L, Simard LR. Survival motor neuron (SMN) protein: Role in neurite outgrowth and neuromuscular maturation during neuronal differentiation and development. Hum Mol Genet 2002;11(14):1605-1614.
(66) Zhang HL, Pan F, Hong D, Shenoy SM, Singer RH, Bassell GJ. Active transport of the survival motor neuron protein and the role of exon-7 in cytoplasmic localization. Journal of Neuroscience 2003;23(16):6627-6637.
(67) Zhang H, Xing L, Rossoll W, Wichterle H, Singer RH, Bassell GJ. Multiprotein complexes of the survival of motor neuron protein SMN with Gemins traffic to neuronal processes and growth cones of motor neurons. Journal of Neuroscience 2006;26(33):8622-8632.
(68) Rossoll W, Jablonka S, Andreassi C, Kröning A-K, Karle K, Monani UR, et al. Smn, the spinal muscular atrophy-determining gene product, modulates axon growth and localization of β-actin mRNA in growth cones of motoneurons. J Cell Biol 2003;163(4):801-812.
(69) Rossoll W, Kröning A-K, Ohndorf U-M, Steegborn C, Jablonka S, Sendtner M. Specific interaction of Smn, the spinal muscular atrophy determining gene product, with hnRNP-R and gry-rbp/hnRNP-Q: A role for Smn in RNA processing in motor axons? Hum Mol Genet 2002;11(1):93-105.
(70) Ting C-H, Wen H-L, Liu H-C, Hsieh-Li H, Li H, Lin-Chao S. The Spinal Muscular Atrophy Disease Protein SMN Is Linked to the Golgi Network. PLoS ONE 2012;7(12).
(71) Fallini C, Zhang H, Su Y, Silani V, Singer RH, Rossoll W, et al. The Survival of Motor Neuron (SMN) protein interacts with the mRNA-binding protein HuD and regulates localization of poly(A) mRNA in primary motor neuron axons. Journal of Neuroscience 2011;31(10):3914-3925.
(72) McWhorter ML, Monani UR, Burghes AHM, Beattie CE. Knockdown of the survival motor neuron (Smn) protein in zebrafish causes defects in motor axon outgrowth and pathfinding. J Cell Biol 2003;162(5):919-931.
(73) McGovern VL, Gavrilina TO, Beattie CE, Burghes AHM. Embryonic motor axon development in the severe SMA mouse. Hum Mol Genet 2008;17(18):2900-2909.
(74) Sanchez G, Dury AY, Murray LM, Biondi O, Tadesse H, El Fatimy R, et al. A novel function for the survival motoneuron protein as a translational regulator. Hum Mol Genet 2013;22(4):668-684.
(75) Hubers L, Valderrama-Carvajal H, Laframboise J, Timbers J, Sanchez G, Côté J. HuD

interacts with survival motor neuron protein and can rescue spinal muscular atrophy-like neuronal defects. Hum Mol Genet 2011;20(3):553-579.
(76) Bowerman M, Shafey D, Kothary R. Smn depletion alters profilin II expression and leads to upregulation of the RhoA/ROCK pathway and defects in neuronal integrity. Journal of Molecular Neuroscience 2007;32(2):120-131.
(77) Bowerman M, Anderson CL, Beauvais A, Boyl PP, Witke W, Kothary R. SMN, profilin IIa and plastin 3: A link between the deregulation of actin dynamics and SMA pathogenesis. Molecular and Cellular Neuroscience 2009;42(1):66-74.
(78) Murray LM, Comley LH, Thomson D, Parkinson N, Talbot K, Gillingwater TH. Selective vulnerability of motor neurons and dissociation of pre- and post-synaptic pathology at the neuromuscular junction in mouse models of spinal muscular atrophy. Hum Mol Genet 2008;17(7):949-962.
(79) Murray LM, Beauvais A, Bhanot K, Kothary R. Defects in neuromuscular junction remodelling in the Smn2B/- mouse model of spinal muscular atrophy. Neurobiol Dis 2013;49(1):57-67.
(80) Goulet BB, Kothary R, Parks RJ. At the "junction" of spinal muscular atrophy pathogenesis: The role of neuromuscular junction dysfunction in SMA disease progression. Curr Mol Med 2013;13(7):1160-1174.
(81) Chang HC-, Dimlich DN, Yokokura T, Mukherjee A, Kankel MW, Sen A, et al. Modeling spinal muscular atrophy in Drosophila. PLoS ONE 2008;3(9).
(82) Novelli G, Calzà L, Amicucci P, Giardino L, Pozza M, Silani V, et al. Expression study of survival motor neuron gene in human fetal tissues. Biochem Mol Med 1997;61(1):102-106
(83) La Bella V, Kallenbach S, Pettmann B. Post-translational modifications in the survival motor neuron protein. Biochem Biophys Res Commun 2004;324(1):288-293.
(84) Soler-Botija C, Cuscò I, Caselles L, Lòpez E, Baiget M, Tizzano EF. Implication of fetal SMN2 expression in type I SMA pathogenesis: Protection or pathological gain of function? J Neuropathol Exp Neurol 2005;64(3):215-223.
(85) Rudnik-Schöneborn S, Heller R, Berg C, Betzler C, Grimm T, Eggermann T, et al. Congenital heart disease is a feature of severe infantile spinal muscular atrophy. J Med Genet 2008;45(10):635-638.
(86) Shababi M, Glascock J, Lorson CL. Combination of SMN trans-splicing and a neurotrophic factor increases the life span and body mass in a severe model of spinal muscular atrophy. Hum Gene Ther 2011;22(2):135-144.
(87) Bevan AK, Hutchinson KR, Foust KD, Braun L, McGovern VL, Schmelzer L, et al. Early heart failure in the SMNΔ7 model of spinal muscular atrophy and correction by postnatal scAAV9-SMN delivery. Hum Mol Genet 2010;19(20):3895-3905.
(88) Heier CR, Satta R, Lutz C, Didonato CJ. Arrhythmia and cardiac defects are a feature of spinal muscular atrophy model mice. Hum Mol Genet 2010;19(20):3906-3918.
(89) Palladino A, Passamano L, Taglia A, D'Ambrosio P, Scutifero M, Cecio MR, et al. Cardiac involvement in patients with spinal muscular atrophies. Acta Myologica 2011;30:175-178.
(90) Bach JR, Saltstein K, Sinquee D, Weaver B, Komaroff E. Long-term survival in Werdnig-Hoffmann disease. American Journal of Physical Medicine and Rehabilitation 2007;86(5):339-345.
(91) Hachiya Y, Arai H, Hayashi M, Kumada S, Furushima W, Ohtsuka E, et al. Autonomic dysfunction in cases of spinal muscular atrophy type 1 with long survival. Brain and Development 2005;27(8):574-578.
(92) Araujo A, Araujo M, Swoboda KJ. Vascular Perfusion Abnormalities in Infants with Spinal Muscular Atrophy. J Pediatr 2009;155(2):292-294.

(93) Martínez-Hernández R, Soler-Botija C, Also E, Alias L, Caselles L, Gich I, et al. The developmental pattern of myotubes in spinal muscular atrophy indicates prenatal delay of muscle maturation. J Neuropathol Exp Neurol 2009;68(5):474-481.
(94) Shafey D, Côté PD, Kothary R. Hypomorphic Smn knockdown C2C12 myoblasts reveal intrinsic defects in myoblast fusion and myotube morphology. Exp Cell Res 2005;311(1):49-61.
(95) Ling KKY, Gibbs RM, Feng Z, Ko C-P. Severe neuromuscular denervation of clinically relevant muscles in a mouse model of spinal muscular atrophy. Hum Mol Genet 2012;21(1):185-195.
(96) Hayhurst M, Wagner AK, Cerletti M, Wagers AJ, Rubin LL. A cell-autonomous defect in skeletal muscle satellite cells expressing low levels of survival of motor neuron protein. Dev Biol 2012;368(2):323-334.
(97) Crawford TO, Sladky JT, Hurko O, Besner-Johnston A, Kelley RI. Abnormal fatty acid metabolism in childhood spinal muscular atrophy. Ann Neurol 1999;45(3):337-343.
(98) Bowerman M, Swoboda KJ, Michalski J-P, Wang G-S, Reeks C, Beauvais A, et al. Glucose metabolism and pancreatic defects in spinal muscular atrophy. Ann Neurol 2012;72(2):256-268.
(99) Le TT, McGovern VL, Alwine IE, Wang X, Massoni-Laporte A, Rich MM, et al. Temporal requirement for high SMN expression in SMA mice. Hum Mol Genet 2011;20(18):3578-3591.
(100) Hua Y, Sahashi K, Rigo F, Hung G, Horev G, Bennett CF, et al. Peripheral SMN restoration is essential for long-term rescue of a severe spinal muscular atrophy mouse model. Nature 2011;478(7367):123-126.
(101) Chang J-G, Hsieh-Li H, Jong Y-J, Wang NM, Tsai C-H, Li H. Treatment of spinal muscular atrophy by sodium butyrate. Proc Natl Acad Sci U S A 2001;98(17):9808-9813.
(102) Sumner CJ, Huynh TN, Markowitz JA, Perhac JS, Hill B, Coovert DD, et al. Valproic Acid Increases SMN Levels in Spinal Muscular Atrophy Patient Cells. Ann Neurol 2003;54(5):647-654.
(103) Brichta L, Hofmann Y, Hahnen E, Siebzehnrubi FA, Raschke H, Blumcke I, et al. Valproic acid increases the SMN2 protein level: A well-known drug as a potential therapy for spinal muscular atrophy. Hum Mol Genet 2003;12(19):2481-2489.
(104) Weihl CC, Connolly AM, Pestronk A. Valproate may improve strength and function in patients with type III/IV spinal muscle atrophy. Neurology 2006;67(3):500-501.
(105) Swoboda KJ, Scott CB, Reyna SP, Prior TW, LaSalle B, Sorenson SL, et al. Phase II open label study of valproic acid in spinal muscular atrophy. PLoS ONE 2009;4(5).
(106) Swoboda KJ, Scott CB, Crawford TO, Simard LR, Reyna SP, Krosschell KJ, et al. SMA CARNI-VAL trial part I: Double-blind, randomized, placebo-controlled trial of L-carnitine and valproic acid in spinal muscular atrophy. PLoS ONE 2010;5(8).
(107) Garbes L, Heesen L, Hölker I, Bauer T, Schreml J, Zimmermann K, et al. VPA response in SMA is suppressed by the fatty acid translocase CD36. Hum Mol Genet 2013;22(2):398-407.
(108) Pane M, Staccioli S, Messina S, D'Amico A, Pelliccioni M, Mazzone ES, et al. Daily salbutamol in young patients with SMA type II. Neuromuscular Disorders 2008;18(7):536-540.
(109) Tiziano FD, Lomastro R, Pinto AM, Messina S, D'Amico A, Fiori S, et al. Salbutamol increases survival motor neuron (SMN) transcript levels in leucocytes of spinal muscular atrophy (SMA) patients: Relevance for clinical trial design. J Med Genet 2010;47(12):856-858.
(110) Farooq F, Molina FA, Hadwen J, MacKenzie D, Witherspoon L, Osmond M, et al. Prolactin increases SMN expression and survival in a mouse model of severe spinal muscular atrophy via the STAT5 pathway. J Clin Invest 2011;121(8):3042-3050.
(111) Meyer K, Marquis J, Trüb J, Nlend Nlend R, Verp S, Ruepp M-, et al. Rescue of a severe mouse model for spinal muscular atrophy by U7 snRNA-mediated splicing modulation. Hum Mol Genet 2009;18(3):546-555.

(112) Coady TH, Shababi M, Tullis GE, Lorson CL. Restoration of SMN function: Delivery of a trans-splicing RNA Re-directs SMN2 pre-mRNA splicing. Molecular Therapy 2007;15(8):1471-1478.
(113) Coady TH, Lorson CL. Trans-splicing-mediated improvement in a severe mouse model of spinal muscular atrophy. Journal of Neuroscience 2010;30(1):126-130.
(114) Hua Y, Vickers TA, Okunola HL, Bennett CF, Krainer AR. Antisense Masking of an hnRNP A1/A2 Intronic Splicing Silencer Corrects SMN2 Splicing in Transgenic Mice. Am J Hum Genet 2008;82(4):834-848.
(115) Hua Y, Sahashi K, Hung G, Rigo F, Passini MA, Bennett CF, et al. Antisense correction of SMN2 splicing in the CNS rescues necrosis in a type III SMA mouse model. Genes and Development 2010;24(15):1634-1644.
(116) Passini MA, Bu J, Roskelley EM, Richards AM, Sardi SP, O'Riordan CR, et al. CNS-targeted gene therapy improves survival and motor function in a mouse model of spinal muscular atrophy. J Clin Invest 2010;120(4):1253-1264.
(117) Dolgin E. Call in the backup. Nat Med 2012;18(11):1602-1606.
(118) Le TT, Pham LT, Butchbach MER, Zhang HL, Monani UR, Coovert DD, et al. SMNΔ7, the major product of the centromeric survival motor neuron (SMN2) gene, extends survival in mice with spinal muscular atrophy and associates with full-length SMN. Hum Mol Genet 2005;14(6):845-857.
(119) Heier CR, DiDonato CJ. Translational readthrough by the aminoglycoside geneticin (G418) modulates SMN stability in vitro and improves motor function in SMA mice in vivo. Hum Mol Genet 2009;18(7):1310-1322.
(120) Mattis VB, Ebert AD, Fosso MY, Chang C-W, Lorson CL. Delivery of a read-through inducing compound, TC007, lessens the severity of a spinal muscular atrophy animal model. Hum Mol Genet 2009;18(20):3906-3913.
(121) Mattis VB, Chang C-W, Lorson CL. Analysis of a read-through promoting compound in a severe mouse model of spinal muscular atrophy. Neurosci Lett 2012;525(1):72-75.
(122) Rothstein JD, Patel S, Regan MR, Haenggeli C, Huang YH, Bergles DE, et al. β-Lactam antibiotics offer neuroprotection by increasing glutamate transporter expression. Nature 2005;433(7021):73-77.
(123) Rothstein JD, Jin L, Dykes-Hoberg M, Kuncl RW. Chronic inhibition of glutamate uptake produces a model of slow neurotoxicity. Proc Natl Acad Sci U S A 1993;90(14):6591-6595.
(124) Nizzardo M, Nardini M, Ronchi D, Salani S, Donadoni C, Fortunato F, et al. Beta-lactam antibiotic offers neuroprotection in a spinal muscular atrophy model by multiple mechanisms. Exp Neurol 2011;229(2):214-225.
(125) Vardatsikos G, Sahu A, Srivastava AK. The insulin-like growth factor family: Molecular mechanisms, redox regulation, and clinical implications. Antioxidants and Redox Signaling 2009;11(5):1165-1190.
(126) Tsai L-K, Chen Y-C, Cheng W-C, Ting C-H, Dodge JC, Hwu W-L, et al. IGF-1 delivery to CNS attenuates motor neuron cell death but does not improve motor function in type III SMA mice. Neurobiol Dis 2012;45(1):272-279.
(127) Bosch-Marcé M, Wee CD, Martinez TL, Lipkes CE, Choe DW, Kong L, et al. Increased IGF-1 in muscle modulates the phenotype of severe SMA mice. Hum Mol Genet 2011;20(9):1844-1853.
(128) Murdocca M, Malgieri A, Luchetti A, Saieva L, Dobrowolny G, de Leonibus E, et al. IPLEX administration improves motor neuron survival and ameliorates motor functions in a severe mouse model of spinal muscular atrophy. Molecular Medicine 2012;18(7):1076-1085.
(129) Bowerman M, Beauvais A, Anderson CL, Kothary R. Rho-kinase inactivation prolongs

survival of an intermediate SMA mouse model. Hum Mol Genet 2010;19(8):1468-1478.
(130) Bowerman M, Murray LM, Boyer JG, Anderson CL, Kothary R. Fasudil improves survival and promotes skeletal muscle development in a mouse model of spinal muscular atrophy. BMC Medicine 2012;10.
(131) Corti S, Nizzardo M, Nardini M, Donadoni C, Salani S, Ronchi D, et al. Neural stem cell transplantation can ameliorate the phenotype of a mouse model of spinal muscular atrophy. J Clin Invest 2008;118(10):3316-3330.
(132) Corti S, Nizzardo M, Nardini M, Donadoni C, Salani S, Ronchi D, et al. Embryonic stem cell-derived neural stem cells improve spinal muscular atrophy phenotype in mice. Brain 2010;133(2):465-481.
(133) Azzouz M, Le T, Ralph GS, Walmsley L, Monani UR, Lee DCP, et al. Lentivector-mediated SMN replacement in a mouse model of spinal muscular atrophy. J Clin Invest 2004;114(12):1726-1731.
(134) Boutin S, Monteilhet V, Veron P, Leborgne C, Benveniste O, Montus MF, et al. Prevalence of serum IgG and neutralizing factors against adeno-associated virus (AAV) types 1, 2, 5, 6, 8, and 9 in the healthy population: Implications for gene therapy using AAV vectors. Hum Gene Ther 2010;21(6):704-712.
(135) Futaki S, Suzuki T, Ohashi W, Yagami T, Tanaka S, Ueda K, et al. Arginine-rich peptides. An abundant source of membrane-permeable peptides having potential as carriers for intracellular protein delivery. J Biol Chem 2001;276(8):5836-5840.
(136) Palm-Apergi C, Lönn P, Dowdy SF. Do cell-penetrating peptides actually penetrate cellular membranes? Molecular Therapy 2012;20(4):695-697.
(137) Frankel AD, Pabo CO. Cellular uptake of the tat protein from human immunodeficiency virus. Cell 1988;55(6):1189-1193.
(138) Vivès E, Brodin P, Lebleu B. A truncated HIV-1 Tat protein basic domain rapidly translocates through the plasma membrane and accumulates in the cell nucleus. J Biol Chem 1997;272(25):16010-16017.
(139) Schwarze SR, Ho A, Vocero-Akbani A, Dowdy SF. In vivo protein transduction: Delivery of a biologically active protein into the mouse. Science 1999;285(5433):1569-1572.
(140) Van de Waterbeemd H, Camenisch G, Folkers G, Chretien JR, Raevsky OA. Estimation of blood-brain barrier crossing of drugs using molecular size and shape, and H-bonding descriptors. J Drug Target 1998;6(2):151-165.
(141) Cao G, Pei W, Ge H, Liang Q, Luo Y, Sharp FR, et al. In vivo delivery of a Bcl-xL fusion protein containing the TAT protein transduction domain protects against ischemic brain injury and neuronal apoptosis. Journal of Neuroscience 2002;22(13):5423-5431.
(142) Sonnemann KJ, Heun-Johnson H, Turner AJ, Baltgalvis KA, Lowe DA, Ervasti JM. Functional substitution by TAT-utrophin in dystrophin-deficient mice. PLoS Medicine 2009;6(5).
(143) Flinterman M, Farzaneh F, Habib N, Malik F, Gäken J, Tavassoli M. Delivery of therapeutic proteins as secretable TAT fusion products. Molecular Therapy 2009;17(2):334-342.
(144) Poulin KL, Lanthier RM, Smith AC, Christou C, Quiroz MR, Powell KL, et al. Retargeting of adenovirus vectors through genetic fusion of a single-chain or single-domain antibody to capsid protein IX. J Virol 2010;84(19):10074-10086.
(145) Chartier C, Degryse E, Gantzer M, Dieterlé A, Pavirani A, Mehtali M. Efficient generation of recombinant adenovirus vectors by homologous recombination in Escherichia coli. J Virol 1996;70(7):4805-4810.
(146) Ross PJ, Parks RJ. Construction and characterization of adenovirus vectors. Cold Spring Harbor Protocols 2009;4(5).
(147) Shaw PA, Catchpole IR, Goddard CA, Colledge WH. Comparison of protein transduction

domains in mediating cell delivery of a secreted CRE protein. Biochemistry 2008;47(4):1157-1166.
(148) Goulet BB, McFall ER, Wong CM, Kothary R, Parks RJ. Supraphysiological expression of survival motor neuron protein from an adenovirus vector does not adversely affect cell function. Biochemistry and Cell Biology 2013;91(4):252-264.
(149) DiDonato CJ, Lorson CL, De Repentigny Y, Simard L, Chartrand C, Androphy EJ, et al. Regulation of murine survival motor neuron (Smn) protein levels by modifying Smn exon 7 splicing. Hum Mol Genet 2001;10(23):2727-2736.
(150) Schmidt PM, Sparrow LG, Attwood RM, Xiao X, Adams TE, McKimm-Breschkin J. Taking down the FLAG! how insect cell expression challenges an established tag-system. PLoS ONE 2012;7(6).
(151) Shen Y, Yu W, Hay JG, Sauthoff H. Expressed cell-penetrating peptides can induce a bystander effect, but passage through the secretory pathway reduces protein transduction activity. Molecular Therapy 2011;19(5):903-912.
(152) Peter CJ, Evans M, Thayanithy V, Taniguchi-Ishigaki N, Bach I, Kolpak A, et al. The COPI vesicle complex binds and moves with survival motor neuron within axons. Hum Mol Genet 2011;20(9):1701-1711.
(153) Klausner RD, Donaldson JG, Lippincott-Schwartz J. Brefeldin A: Insights into the control of membrane traffic and organelle structure. J Cell Biol 1992;116(5):1071-1080.

# JOSEPH BURNS

## EDUCATION

Sept. 2011 – Present University of Ottawa, Ottawa, ON
*Master of Science, Biochemistry with Specialization in Human and Molecular Genetics*

Sept. 2006 – April 2011 University of Ottawa, Ottawa, ON
*Honours Bachelor of Science with Specialization in Biochemistry, CO-OP*

Sept. 2002 – June 2006 St. Patrick's High School, Sarnia, ON
*Ontario Secondary School Diploma*

## WORK EXPERIENCE

Sept. 2011 – Present Ottawa Hospital Research Institute, Ottawa, ON
*M.Sc. Student (Parks Lab)*

- Assisted with direction of a project concerning a protein therapy approach for spinal muscular atrophy
- Generated and purified large-scale fusion protein preparations using *E. coli*
- Performed transfections and protein transductions to evaluate fusion proteins *in vitro*
- Developed and refined a protocol for recovering secreted fusion proteins from media
- Regularly performed SDS-PAGE and Western blots
- Maintained multiple mammalian cell lines
- Thesis successfully defended Feb. 10, 2014

Sept. 2010 – April 2011 Ottawa Hospital Research Institute, Ottawa, ON
*Honours Project Student (Parks Lab)*

- Cloned constructs of a reporter protein with various added domains affecting membrane permeability and secretion
- Acquired familiarity with transfections, fluorescence microscopy, and protein harvest
- Purified and assessed proteins for capability for transduction and/or secretion

May 2010 – August 2010 Spartan Bioscience, Inc., Ottawa, ON

*Co-op Student*

- Received NSERC Industrial Undergraduate Student Research Award
- Optimized qPCR protocols and assisted with shaping project direction
- Assisted with unit validation for a PCR-based clinical trial
- Performed gel electrophoresis to verify PCR results
- Composed a full report for each experiment performed

Jan. 2009 – Dec. 2009 Ottawa Regional Cancer Centre, Ottawa, ON

*Co-op Student (Bell Lab)*

- Performed quantitative PCR and immunohistochemistry on human tumour biopsies for an oncolytic virus clinical trail resulting in a collaborative publication in Nature
- Conducted experiments evaluating the effects of chemotherapy drugs on viral infection and replication
- Improved qPCR skills by performing a biodistribution of virus in mouse tissues
- Maintained cell lines for *in vitro* experiments
- Incubated and titrated virus stocks and virus-infected cell samples
- Received classroom and hands-on training with mice including handling and injection procedures

## SKILLS

- Tissue culture including transfections, infections, harvests and timepoints
- PCR and qPCR
- Detection and quantification of viral particles in cells and tissue samples
- Cloning and induction of protein expression in bacteria
- SDS-PAGE, Western blots, Coomassie staining, and agarose gel electrophoresis
- Composition of laboratory reports and literature reviews
- Critical analysis and presentation of literature and of my data
- Fluent in English, moderate skills in French, basic Japanese
- Confident with computer software such as word processors, spreadsheets, and presentation software

## AWARDS

At University of Ottawa:

- Queen Elizabeth II Graduate Scholarship in Science and Technology (2011-2013)
- University of Ottawa Excellence Scholarship (Graduate)
- University of Ottawa Admission Scholarship (Undergraduate)
- Dean’s Honour List for the years 2007-2008, 2008-2009, 2009-2010, 2010-2011
- Queen Elizabeth II Aiming for the Top Scholarship
- University of Ottawa Student Mobility Scholarship
- NSERC Industrial Undergraduate Student Research Award

At St. Patrick's High School:

- Governor General’s Academic Medal
- Ontario Scholar Certificate - Highest Average

- Colt Engineering Physics, Mathematics, and Chemistry Award
- IODE Elizabeth II Chapter English Award

## PUBLICATIONS AND PRESENTATIONS

*The role of chromatin in adenoviral function*

C.M. Wong, E.R. McFall, **J.K. Burns,** and R.J. Parks

*Viruses,* 5(6): 1500-1515. June 2013

*The oncolytic poxvirus JX-594 selectively replicates in and destroys cancer cells driven by genetic pathways commonly activated in cancers*

K.A. Parato, C.J. Breitbach, F. Le Boeuf, J. Wang, C. Storbeck, C. Ilkow, J.-S. Diallo, T. Falls, **J. Burns**, V. Garcia, F. Kanji, L. Evgin, K. Hu, F. Paradis, S. Knowles, T.-H. Hwang, B.C. Vanderhyden, R. Auer, D.H. Kirn, and J.C. Bell

*Molecular Therapy,* 20(4): 749-758. April 2012

*Intravenous delivery of a multi-mechanistic cancer-targeted oncolytic poxvirus in humans*

C.J. Breitbach, J. Burke, D. Jonker, J. Stephenson, A.R. Haas, L.Q.M. Chow, J. Nieva, T. Hwang, A. Moon, R. Patt, A. Pelusio, F. Le Boeuf, **J. Burns**, L. Evgin, N. De Silva, S. Cvancic, T. Robertson, J. Je, Y. Lee, K. Parato, J. Diallo, A. Fenster, M. Daneshmand, J.C. Bell, and D.H. Kirn.

*Nature*, 477: 99-104. September 2011.

*Development of a Protein-Based Therapy for Treatment of Spinal Muscular Atrophy*

**Joe Burns,** Rashmi Kothary, and Robin J. Parks

BMI Graduate Poster Day, University of Ottawa, May 2012
OHRI Research Day, November 2012
BMI Graduate Seminar Day, University of Ottawa, March 2013

*Preliminary Studies to Develop a Protein-Based Therapy for Treatment of Spinal Muscular Atrophy*

**Joe Burns** and Robin J. Parks

Biochemistry Undergraduate Research Poster Day, University of Ottawa, April 2011
OHRI Research Day, November 2011